Origin of Thermogenic and Biogenic Natural Gas in the Tongue River Member Coals of the Fort Union Formation, Northeastern Powder River Basin, Wyoming

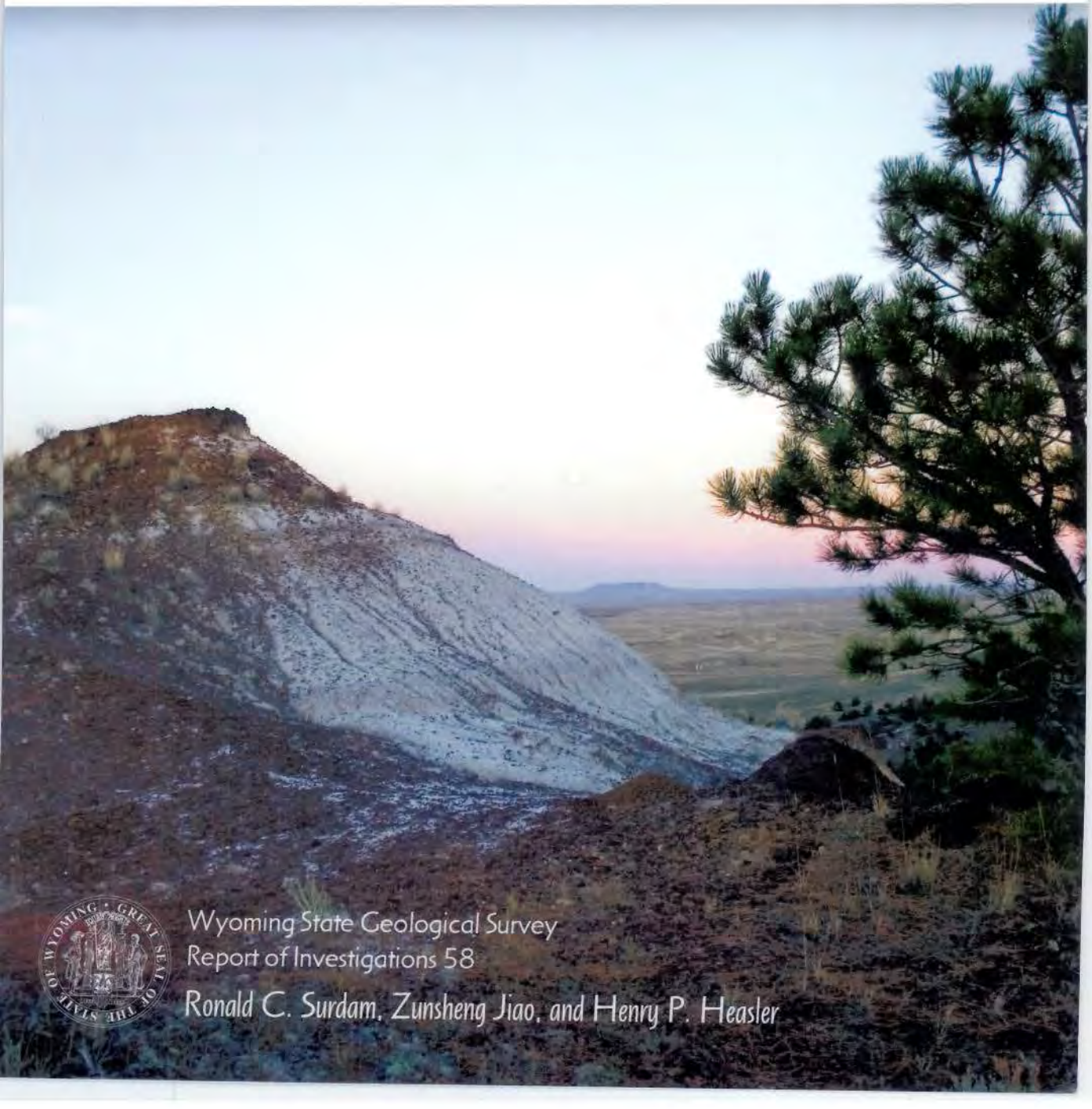

Wyoming State Geological Survey
Report of Investigations 58

Ronald C. Surdam, Zunsheng Jiao, and Henry P. Heasler

Wyoming State Geological Survey
Ronald C. Surdam, State Geologist

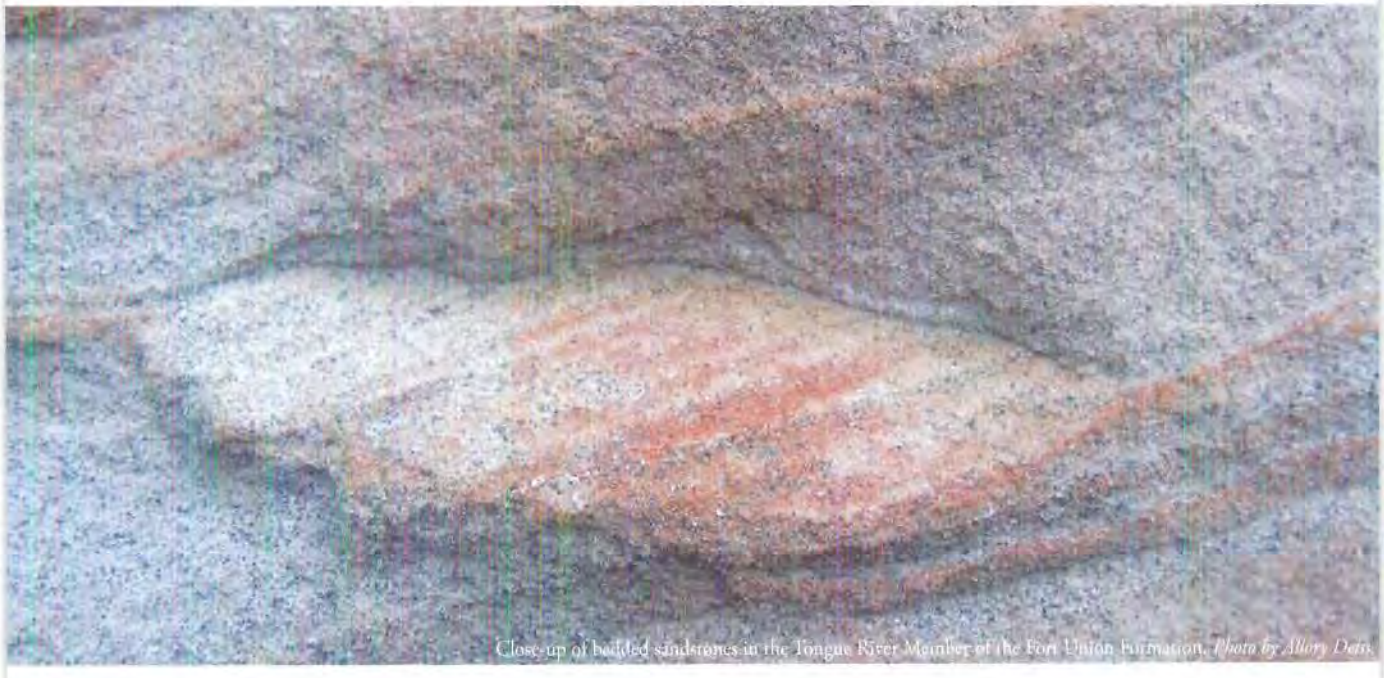

Close-up of bedded sandstones in the Tongue River Member of the Fort Union Formation. *Photo by Allory Deiss.*

First printing of 500 copies by Citizen Printing, Fort Collins, Colorado, November 2007.

Origin of thermogenic and biogenic natural gas in the Tongue River Member coals of the Fort Union Formation, northeastern Powder River Basin, Wyoming, by Ronald C. Surdam, Zunsheng Jiao, and Henry P. Heasler.
Wyoming State Geological Survey Report of Investigations No. 58, 2007.
ISBN 1-884589-44-8

Cover: Outcrop of Tongue River Member looking east to Pumpkin Buttes. *Photo by Meg Ewald.*

Origin of Thermogenic
and Biogenic Natural Gas in the
Tongue River Member Coals of the Fort Union Formation,
Northeastern Powder River Basin, Wyoming

Ronald C. Surdam[1]
Zunsheng Jiao[1]
Henry P. Heasler[2]

[1]Wyoming State Geological Survey
[2]National Park Service, formerly University of Wyoming

TABLE OF CONTENTS

List of Figures

List of Tables

Abstract

This report presents an integrated study of the origin of natural gas in the coal beds of the Tongue River Member, Fort Union Formation located in the Powder River Basin of Wyoming. The origin of natural gas in these coal beds is particularly important because they serve as a source of copious amounts of gas in the form of coalbed natural gas accumulations.

To better understand the source of the coalbed natural gas in the Powder River Basin, we evaluated burial, thermal, and maturation histories and reaction kinetics of hydrocarbon generation in the Tertiary coals and organic-rich shales of the underlying Cretaceous stratigraphic section.

Our evaluations suggest the following conclusions:

- The isotopic composition of natural gas in the Tongue River Member coal beds demonstrates that it is a mixture of thermogenic and biogenic gas.
- The coal beds have had insufficient thermal exposure to generate notable amounts of thermogenic gas.
- During burial, the Tongue River Member coals generated huge quantities of short-chained carboxylic acid and acid anions, providing an ideal environment for methanogenesis (CH_3COOH + bacteria $\rightarrow CH_4 + CO_2$).
- Acetate generation (methanogenesis) in the coals probably began approximately 50 Ma at a burial depth of 500 m, and continued until approximately 10 Ma at a burial depth of 1,000 m.
- At present, the Tongue River Member coals have little or no additional capacity to generate acetate; any acetate available in the coals for methanogenesis was generated in the past, but was not used by methanogenic bacteria.
- The extremely large surface area (combined matrix and fractures) within coal beds provides a multitude of sites for absorption of both biogenic and thermogenic natural gas.
- The thermogenic gas in the coals originated in the underlying organic-rich shales in the more deeply buried Cretaceous stratigraphic section. The source of the biogenic gas in the coals is the coals themselves; this biogenic gas resulted from methanogenesis driven by the in-situ interaction of microbes with a huge quantity of carboxylic acids and acid anions generated during relatively shallow burial (500-1,000 m depth).

Introduction

Thick, lignite to subbituminous (R_0 0.28 to 0.45) coal beds in the Paleocene Tongue River Member of the Fort Union Formation in the Powder River Basin are important sources and reservoirs of natural gas. In order to optimize exploration and develop these important gas resources, it is useful to better understand the generation capability, storage, and fluid migration processes characterizing these coal beds. This study aims to determine the potential for thermogenic and biogenic gas generation from kerogen-rich rocks contained in the Tertiary-Cretaceous stratigraphic section, with specific emphasis on coals of the Tongue River Member located in the Powder River Basin of Wyoming. The study area extends from near the city of Gillette westward to approximately the axis of the Powder River Basin (**Figure 1**). The Tongue River Member of the Fort Union Formation crops out near Gillette, but its base is buried more than 900 meters (2,950 feet) deep at the Cedar Draw well located 29 km (18 miles) to the west (**Figure 2**).

In order to evaluate the possibility of thermogenic gas generation, the temperature history of the coal seams must be estimated as closely as possible. Primary factors influencing the temperature of a geologic unit at a specific time during burial include the amount of heat flowing into the base of the sedimentary sequence, and the thermal conductivity of the individual units of the sedimentary sequence. To calculate the temperature history of a given geologic unit, the burial history of the unit must be estimated also. As described by Waples (1980), important factors influencing burial history are thickness of geologic units, age of geologic units, presence of erosional events, and periods of non-deposition. Erosional events are important because they affect the maximum burial depth of a sedimentary unit (and hence its temperature history), the timing of maximum burial depth, and the maximum temperature of the unit under investigation.

In this report, we describe the methodology and data used to construct temperature histories for various organic-rich units (potential gas sources) in the area of interest. We then use these

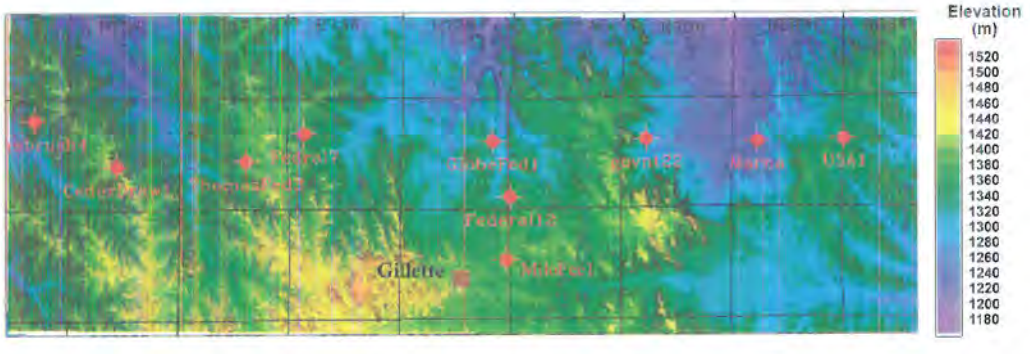

Figure 1. Index map of the study area. The red dots represent wells used to construct the cross section shown in Figure 2. The basin axis is located 32 miles west of the west margin of the figure.

results to calculate potential thermogenic gas generation, and/or carboxylic acid generation (an essential component of biogenesis), in coal beds and organic-rich shales of the Tertiary-Cretaceous stratigraphic section.

The kinetic values used to evaluate the hydrocarbon maturation history of the Tongue River Member were taken from Tissot and Welte (1984) for Type II and Type III kerogens, and were validated "in house" using hydrous pyrolysis experimental techniques. In addition, we determined kinetic values for the reaction of coal to acetate (derived by cleaving oxygen-bearing functional groups from kerogen) using hydrous pyrolysis techniques. Using published and experimentally-derived kinetics along with constructed temperature histories allows the modeling and evaluation of the conversion of kerogen in coals to both hydrocarbons and acetate (feedstock for bacteria involved in methanogenesis).

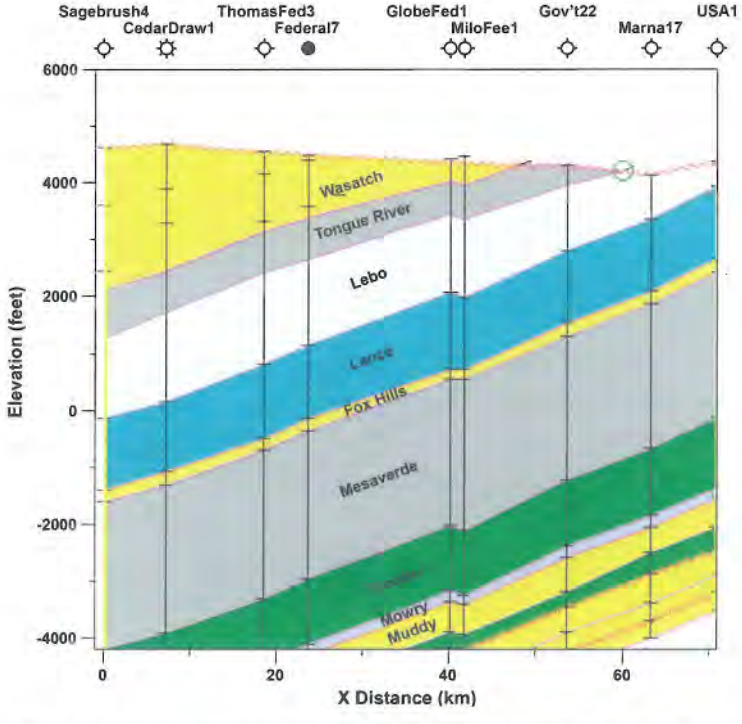

Figure 2. An east-west stratigraphic section through the study area. The Tongue River Member of the Fort Union Formation crops out near Gillette, Wyoming, but its base is buried more than 900 meters (2,950 feet) deep at the Cedar Draw well.

Burial History Reconstruction

The data contained in **Figure 2** represent the present depths and thicknesses of sedimentary units of interest along the cross section formed by the wells shown in **Figure 1**. The data were gathered from interpretation of electric well logs and Petroleum Information cards on file at the Wyoming State Geological Survey and Wyoming Oil and Gas Conservation Commission. We used these data in the burial history construction in order to constrain the thickness of units and present-day depths. We also used **Figure 2** to establish present-day minimum (Milo Fee 1 well) and maximum (Cedar Draw 1 well) burial cases for the Tongue River Member.

Ages of the various sedimentary units were taken from the RMAG Geologic Atlas of the Rocky Mountain Region (1972). Using these age dates, thicknesses, and present-day depths of units of interest, preliminary burial histories can be constructed. The Powder River Basin experienced a major Tertiary erosional event, as have other Wyoming intermountain basins (Mackin, 1937; Van Houton, 1952; Love, 1960, 1970). Mackin (1937), Van Houten (1952), and Love (1960) reported that the pre-erosional Tertiary surface in the adjacent Bighorn Basin existed at an elevation of 2,740 m (9,000 ft), whereas Sundell (1985) reported the surface at 1,830 to 2,130 m (6,000 to 7,000 ft). The timing of the start of the erosional event in the Bighorn Basin is believed to range from late Eocene (Sundell, 1985) to late Pliocene (Van Houten, 1952; Love, 1960). It has been suggested that the pre-erosional elevation of the Powder River Basin was similar to that of the Bighorn Basin (Buelow et al., 1986). However, the Powder River Basin does not contain a Tertiary volcanic sedimentary section as thick as the section in the Bighorn Basin, and because the Powder River Basin is not encircled by mountains as other Wyoming intermountain basin are, we postulate in this study that the maximum elevation of the pre-erosional surface in the area of Gillette was 2,130 m (7,000 ft).

The lithology and rock property data for the underlying rock units were aggregated to assign geologic age and thermal properties to the stratigraphic section, and to provide additional constraints on the burial history models. The timing of the erosional event was chosen to range from 35 Ma (maximum) to 10 Ma (minimum), with the uplift and erosion characterizing this event continuing today.

In an effort to quantitatively estimate the amount of erosion along the erosional surface, we used a modification of the technique described by Magara (1976). With this technique, it is assumed that the compaction of sediments follows an exponential relationship of the form:

$$\emptyset = \emptyset_0 \, e^{(-Z/b)},$$

where $\emptyset$ is present-day porosity at a given depth Z; $\emptyset_0$ is the porosity at depth Z = 0 (the depositional ground surface); and b is the exponential decay constant (represents the depth interval over which porosity is reduced by the factor 1/e, expressed in unit meters in this report). Many researchers have shown the general validity of an exponential decrease in

porosity with depth (Magara, 1976; Scholle, 1977; Steckler and Watts, 1978; McColloh et al., 1978; Scalater and Christie, 1980). The amount of erosion for a given lithologic unit may be estimated by knowing b, present-day measured porosity Ø, and the depositional porosity value $Ø_0$. By using the functional relationship between present-day measured porosity Ø and the depositional porosity $Ø_0$, the amount of erosion necessary to increase the porosity from the present-day measured Ø to the depositional $Ø_0$ can be quantitatively calculated. This calculated amount of stratigraphic section is equal to the amount of material removed by erosion from the present-day surface.

Magara's technique of estimating erosion using sonic logs is possible because shale compaction relates essentially to overburden load or burial depth. Therefore, if a shale bed is overcompacted for a specific depth, it is interpreted as having been buried more deeply in the geological past and as having lost part of the overburden section to erosion (**Figure 3**). Magara indicates that this method does not apply if the shales are undercompacted. In an undercompacted zone, shale compaction is not a simple function of burial depth. However, no undercompacted shales have been observed in the Powder River Basin.

The level of shale compaction can be determined from the sonic log because sonic transit time is a function of porosity when the fluid content remains water-saturated. The relationship between the logarithm of shale transit time and depth in many sedimentary basins

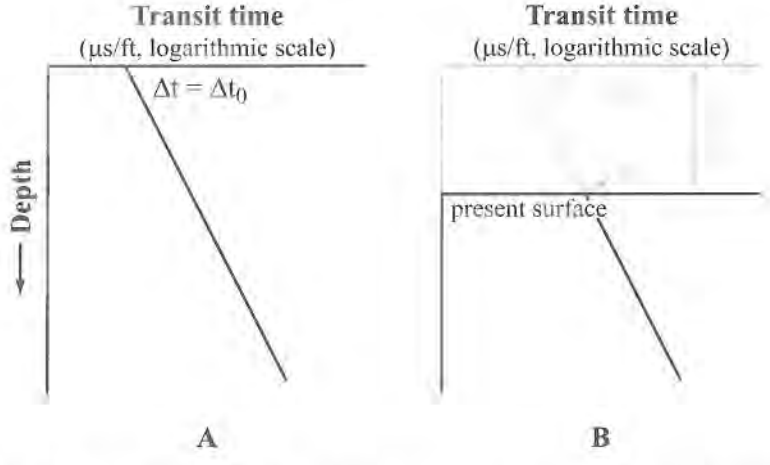

Figure 3. Schematic diagrams showing transit time/depth trends under normal compaction (modified from Magara (1976)). If there has been no significant erosion, the present-day surface transit time Δt will be close to the original deposition-surface transit time Δt_0 (A). However, when there has been a significant erosional event, the present-day surface transit time Δt will be less than the original surface transit time Δt_0 (B). The distance between the present-day surface and the level at which the extrapolated value equals the original deposition-surface transit time Δt_0 (B) is the approximate thickness of sedimentary rocks that have been removed by erosion.

can be approximated by a straight line (Magara, 1976). When extrapolated to the surface, this normal compaction trend gives a surface transit time value Δt for present-day surface rocks. When no significant erosion has occurred, the present-day surface transit time Δt will be close to the original deposition-surface transit time Δt_0 (**Figure 3, A**). However, when a significant erosional event has taken place, the present-day surface transit time Δt will be less than the original surface transit time Δt_0 (**Figure 3, B**). The distance between the present-day surface and the level at which the extrapolated value equals the original deposition-surface transit time Δt_0 (**Figure 3, B**) is equal to the approximate thickness of the sedimentary rock section that has been removed by erosion.

There are two problems with applying Magara's technique to the Powder River Basin. First, Magara's technique was developed based on the properties of shales, but the stratigraphic section of interest in the Powder River Basin is composed of an interbedded sequence of siltstone, shale, and some sandstone. Several authors (Faust, 1951; Cordier, 1985) have demonstrated that clastic sedimentary rocks such as shale and sandstone have a similar trend for transit time versus depth in a normally-compacting sequence. Faust (1951) compared shale velocities and sandstone velocities under similar conditions (similar compaction, fluid composition, and fluid content) and concluded that the velocity difference between the two rock types was small, with sandstone velocity slightly greater. It is assumed that the velocities of sandy shale and shaly sandstone (dominant lithologies in the upper portion of the stratigraphic sequence in the Powder River Basin) lie between the two end members. In this report, we assume that sandstone and shale can be treated as approximately equivalent for the purpose of calculating erosional amounts.

The second problem with Magara's technique relates to choosing the original surface transit time Δt_0 for the Powder River Basin. As shown in **Table 1**, estimated erosion is sensitive to the assumed original surface transit time Δt_0. For example, the Union 3 well (**Table 1**) has an estimated erosion value of approximately 3,300 ft if the original surface transit time is assumed to be 190 µs/ft; however, the estimated erosion value declines to approximately 2,300 ft if the original surface transit time is assumed to be 180 µs/ft. The 1,000-ft erosional difference will significantly affect the reconstruction of the burial and thermal histories.

Table 1. Estimated post-Laramide erosion in the Powder River Basin.

Well name	Location	Erosion amount, ft		
		190 s/ft	180 s/ft	170 s/ft
Roy 12-4	T51N, R69W, Sec 4	4,104	3,358	2,612
Govn't 1	T46N, R70W, Sec 5	3,571	2,857	2,143
Mathes 1	T41N, R69W, Sec 8	4,797	3,984	3,171
Means 21	T46N, R75W, Sec 21	3,154	2,385	1,615
Union 3	T41N, R76W, Sec 23	3,300	2,300	1,300

Transit times in sand- and mud-rich sediments depend greatly on porosity and on the material filling the pores (Faust, 1951; Magara, 1976; Bobrin and Savit, 1988). Depositional porosities are generally in the range of 50% for sandstone and 60% for shale (Baldwin and Butler, 1985). Transit times in clay-rich sediments range from 121 μs/ft to 275 μs/ft, and transit time in loose sand is 165 μs/ft (Bobrin and Savit, 1988). However, under similar conditions, such as the same porosity and pore filling material, sand and clay will have similar transit times (Faust, 1951; Cordier, 1985). To test the sensitivity of the calculation to changes in depositional porosity, erosional amounts were calculated for depositional porosities of 50%, 55%, 60%, 65%, and 70%. A 50% depositional porosity results in 382 m (1,252 ft) of erosion for the Milo Fee 1 well and 0 m of erosion for the Cedar Draw 1 well, and a 55% depositional porosity results in 648 m (2,127 ft) of erosion for the Milo Fee 1 well and 106 m (349 ft) of erosion for the Cedar Draw 1 well.

Based on the empirical relationship between shale porosity and transit time, Magara (1976) reported that the original surface transit time Δt_0 should be between water transit time (200 μs/ft) and matrix transit time (68 μs/ft at 0% porosity), and that the porosity-transit time relationship may be expressed as:

$$\Delta t = (\emptyset + 31.7)/0.466,$$

where Δt is shale transit time (in μs/ft) and $\emptyset$ is shale porosity (in percent).

The youngest rocks in the Powder River Basin (Arikaree Formation or White River Formation) are sandy siltstone deposited in a fluvial environment. After evaluating the petrology and petrography of the interbedded sandstone and mudstone in the Tertiary section of the Powder River Basin, we observed that the depositional porosity of the Tertiary and upper Cretaceous sediments is close to 50-55%. Bond et al. (1983) reported that silty sediments have an average porosity of 52%. Using a porosity value of 52%, we calculated a transit time Δt_0 of 180 μs/ft from Magara's expression. This value, 180 μs/ft, is taken as the original surface transit time for the units of interest in this study. More than 50 wells in the Powder River Basin were used to determine erosional amounts. Assuming 180 μs/ft for the original surface transit time, and using the data in **Table 1**, we estimate that a maximum of 1,000 m (3,280 ft) of erosion has occurred in the portion of the Powder River Basin shown in **Figure 1** and **Figure 2**.

Using the estimated erosional amount, we constructed burial history diagrams for the Milo Fee 1 well and the Cedar Draw 1 well (see **Figure 1** for locations). **Figures 4, 5, and 6** illustrate the burial history of the Milo Fee 1 well for 500 m and 1,000 m of erosion occurring at 10 Ma, and for 1,000 m of erosion occurring at 35 Ma. **Figure 7** illustrates the burial history of the Milo Fee 1 well for 1,000 m of erosion at 35 Ma and a Tertiary thermal conductivity that changes through time due to sediment compaction. **Figures 8, 9, and 10** illustrate the burial history of the Cedar Draw well for 500 m and 1,000 m of erosion at 10 Ma, and for

1,000 m of erosion at 35 Ma. Prior to uplift, the maximum burial depth of the basal Tongue River Member was 1,900 m (6,230 ft) at the Cedar Draw 1 well. Because the Cedar Draw well represents maximum burial of the Tongue River Member in the study area, it is possible to estimate the maximum possible thermal exposure (temperature) for the basal Tongue River Member assuming the maximum erosional case (1,000 m) for either the 35 Ma or 10 Ma erosional events.

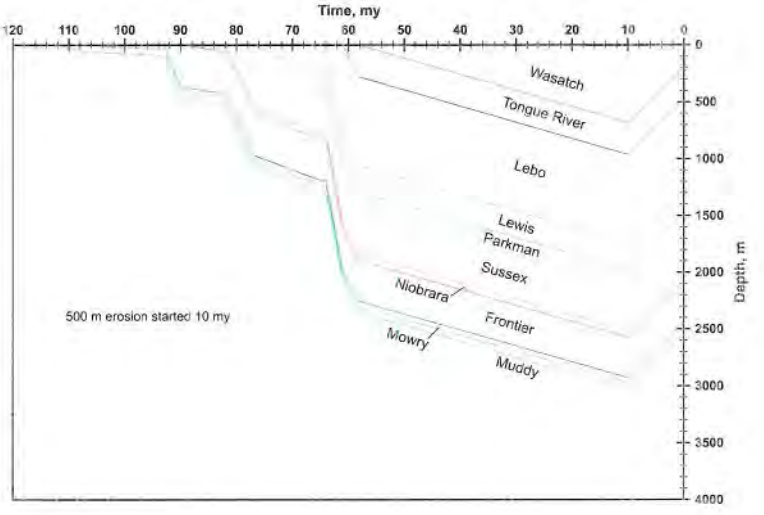

Figure 4. Reconstructed burial history diagram for the Milo Fee 1 well in the study area. The most recent uplift started 10 Ma. An erosional amount of 500 m is used in this reconstruction. The present-day depths were gathered from interpretations of electric well logs and Petroleum Information cards on file at the Wyoming State Geological Survey and Wyoming Oil and Gas Conservation Commission. Ages of the various sedimentary units were taken from the RMAG Geologic Atlas of the Rocky Mountain Region (1972).

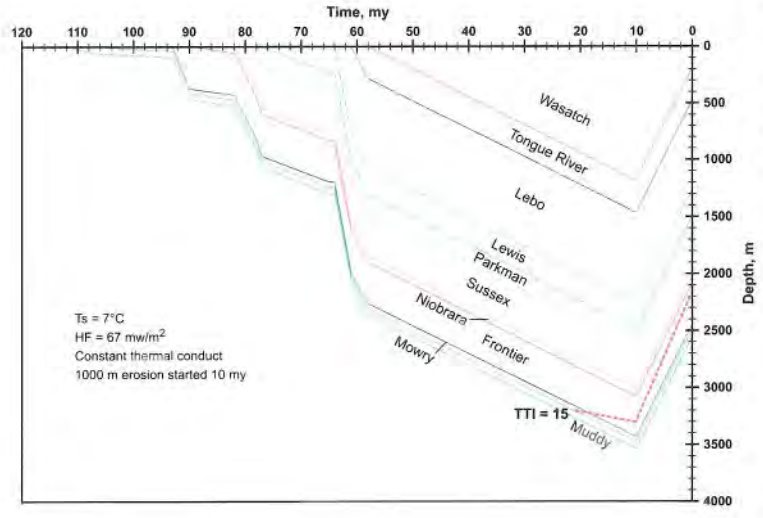

Figure 5. Reconstructed burial history diagram for the Milo Fee 1 well in the study area. The most resent uplift started 10 Ma. An erosional amount of 1,000 m is used in this reconstruction. The time-temperature Index (TTI) value of 15 indicates onset of oil generation (Waples, 1980).

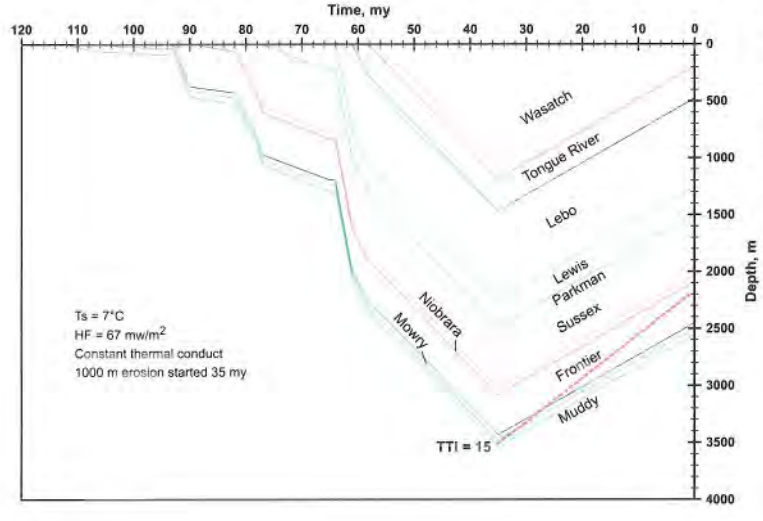

Figure 6. Reconstructed burial history diagram for the Milo Fee 1 well in the study area. The most resent uplift started 35 Ma. An erosional amount of 1,000 m is used in this reconstruction. The time-temperature index (TTI) value of 15 indicates onset of oil generation (Waples, 1980).

Figure 7. Reconstructed burial history diagram for the Milo Fee 1 well in the study area. The most resent uplift started 35 Ma. An erosional amount of 1,000 m is used in this reconstruction. Variable thermal conductivities were used to reconstruct the temperature history. The TTI value of 15 indicates onset of oil generation (Waples, 1980).

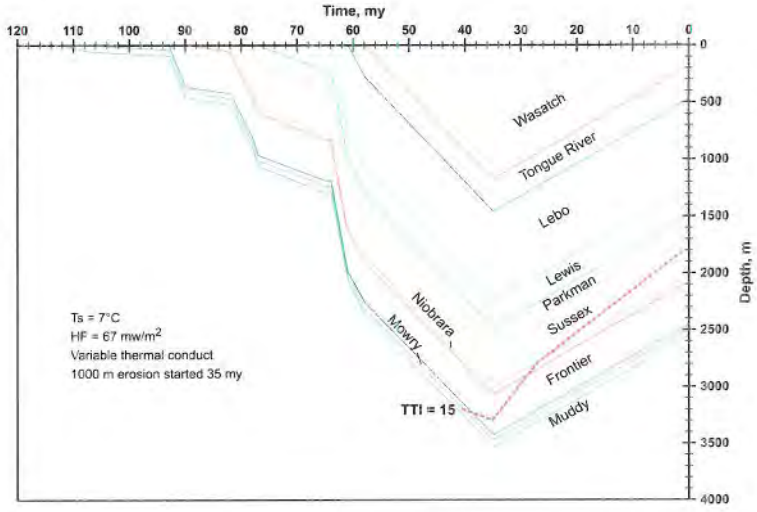

Figure 8. Reconstructed burial history diagram for the Cedar Draw 1 well in the study area. The most resent uplift started 10 Ma. An erosional amount of 500 m is used in this reconstruction.

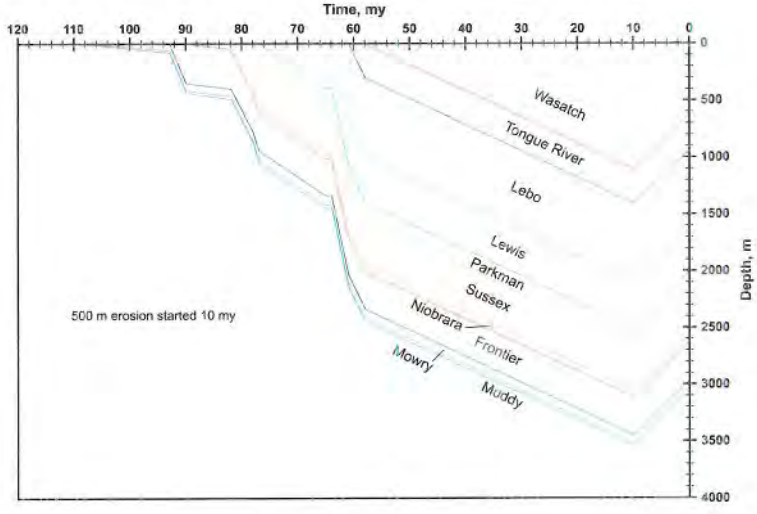

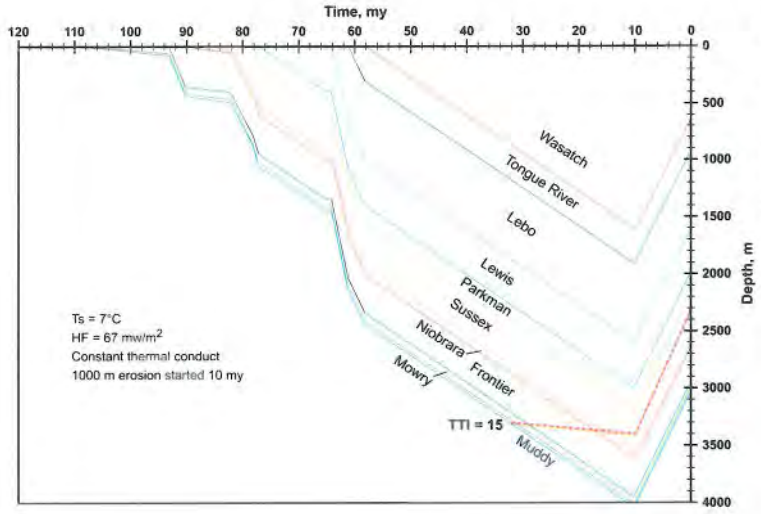

Figure 9. Reconstructed burial history diagram for the Cedar Draw 1 well in the study area. The most resent uplift started 10 Ma. An erosional amount of 1,000 m is used in this reconstruction. The TTI value of 15 indicates onset of oil generation (Waples, 1980).

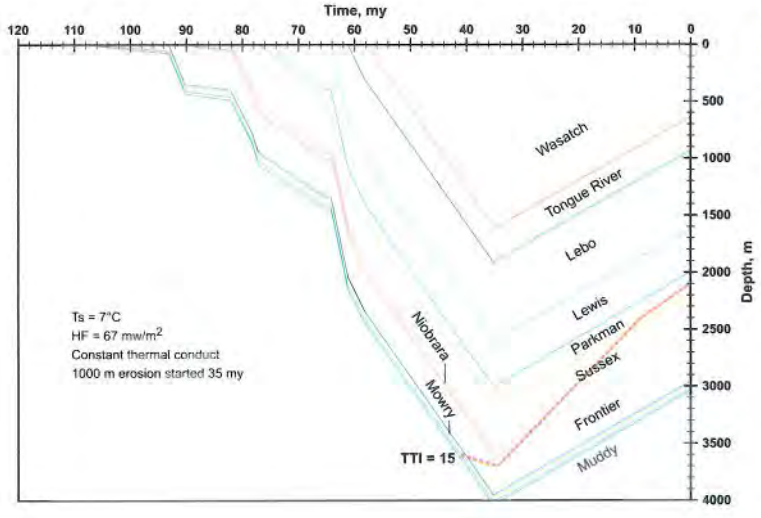

Figure 10. Reconstructed burial history diagram for the Cedar Draw 1 well in the study area. The most resent uplift started 35 Ma. An erosional amount of 1,000 m is used in this reconstruction. The TTI value of 15 indicates onset of oil generation (Waples, 1980).

Thermal Modeling

Given the depths and thicknesses through time of the sedimentary units of interest, a one-dimensional, steady state, conductive thermal model was used to estimate temperature histories. Input parameters for the thermal history modeling include thickness of sedimentary layers, thermal conductivity of sedimentary layers, heat flow into the base of the sedimentary sequence, and ground surface temperature. Temperatures were calculated every 1 million years for the burial histories shown in **Figure 4** through **Figure 10**. The following data were used in the thermal modeling: surface temperature of 7°C (45°F); heat flow of 67×10^{-3} watts/m^2 (Buelow et al. 1986); and thermal conductivities shown in **Table 2**.

Because the Tongue River Member is a primary layer of interest, we constructed a more sophisticated thermal model of the burial histories shown in **Figure 5** and **Figure 7** for the Milo well with 1,000 m of erosion occurring at 10 and 35 Ma, and for the Cedar Draw well as shown in **Figure 9** and **Figure 10** with 1,000 m of erosion occurring at 10 and 35 Ma. In these models, the porosity-depth function was used to calculate a thermal conductivity for the Tertiary section. The thermal conductivity of the Tertiary section should change with compaction (changing ratio of rock to fluid) due to the relative difference in thermal conductivity between the pore-filling fluid (assumed to be water with a thermal conductivity of 0.6 watts/meter•kelvin) and the rock grains (usually in the range of 3.0 to 5.0 watts/meter•kelvin).

Figure 11 shows the effect of changing thickness and burial depth of the stratigraphic units in the Powder River Basin on thermal conductivity. The dotted red line shows the change in thermal conductivity for a thickening wedge of sediments. From **Figure 11**, a 1,000-meter-

Table 2. Layer thermal conductivities for sedimentary units in the Powder River Basin.

Sedimentary unit	Thermal conductivity (watts $meter^{-1}$ $Kelvin^{-1}$)
Wasatch	2.3
Tongue River	2.5
Lebo	2.5
Lewis	1.7
Parkman	2.5
Sussex	2.5
Niobrara	1.7
Frontier	1.9
Mowry	1.7
Muddy	2.9

Values are from Buelow et al., 1986.

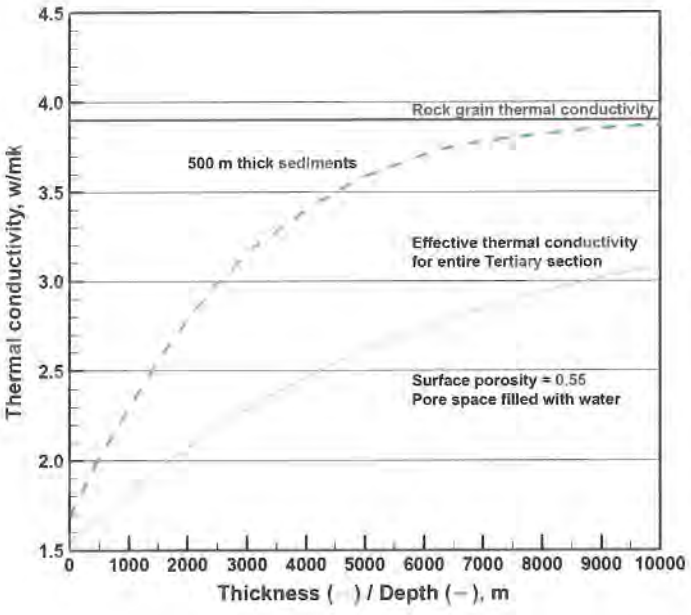

Figure 11. Plot of the calculated thermal conductivities for the Tertiary rocks in the Powder River Basin, Wyoming, showing the effect of thickness and burial depth changes on thermal conductivity of the stratigraphic units of interest. The red dotted line shows the thermal conductivity changing with the unit thickness. The green dashed line shows how the thermal conductivity of the 500-meter-thick sediments changes with progressive burial.

thick sedimentary unit would have a layer thermal conductivity of 1.75 watts/meter•kelvin, whereas a 3,000-meter-thick unit would have a layer conductivity of approximately 2.25 watts/meter•kelvin. If the thermal conductivity of a 500-meter-thick layer is followed during burial, a change similar to that illustrated by the green dashed line in **Figure 11** can be observed. This green dashed line represents the change in layer thermal conductivity for a 500-meter-thick sedimentary unit that is buried from 0 m (thermal conductivity 1.7 watts/meter•kelvin) up to 10,000 m (thermal conductivity 3.9 watts/meter•kelvin). The rock grain thermal conductivity shown in **Figure 11** is the thermal conductivity of the sediment unit at 0% porosity. The value of 3.9 watts/meter•kelvin was chosen for the sediment unit at 0% porosity based on calculation of the green dashed line in **Figure 11**, and on calibration with an oil well bottom-hole temperature reported in Buelow et al. (1986).

Figure 12 shows results of the thermal modeling for the basal Tongue River Member in the Cedar Draw 1 well, including temperature histories of four cases. Cases 1, 2, and 3 correspond to the burial histories shown in **Figure 8**, **Figure 9**, and **Figure 10**. Case 4 corresponds to the burial history shown in **Figure 9**, but with the thermal conductivity of the Tertiary section changing every 10 million years to reflect alterations caused by progressive sediment compaction. Very little difference exists between the maximum predicted temperatures for cases 2, 3, and 4 (all for 1,000 m of erosion). With variable Tertiary thermal conductivity, the temperature at the maximum burial depth reaches 65°C in the basal Tongue River Member at the Cedar Draw well. Because the Cedar Draw well represents the maximum burial scenario for the basal Tongue River Member, it is assumed that the temperatures shown in **Figure 12**

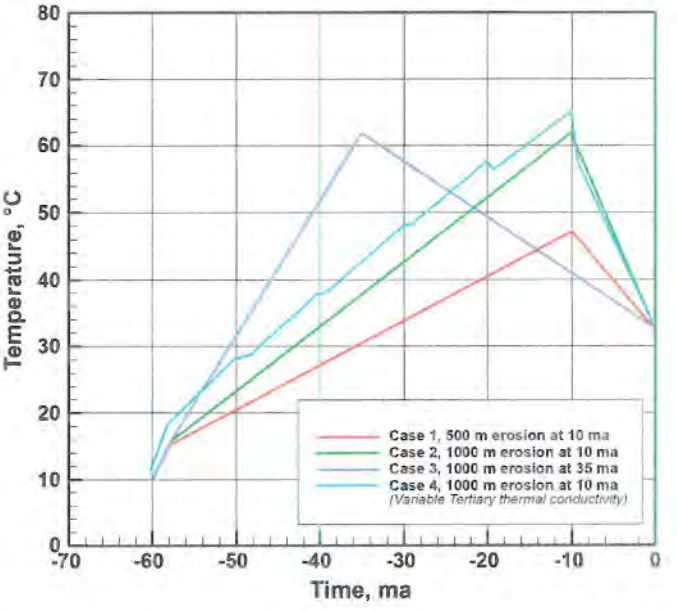

Figure 12. Time-temperature profile for the lower Tongue River Member of the Fort Union Formation at the Cedar Draw 1 well in the study area. Case 1 assumes an erosional amount of 500 m for the most recent erosional event starting 10 Ma. Case 2 assumes an erosional amount of 1,000 m for the most recent erosional event starting 10 Ma. Case 3 assumes an erosional amount of 1,000 m for the most recent erosional event starting 35 Ma. Case 4 assumes an erosional amount of 1,000 m for the most recent erosional event starting 10 Ma. A constant Tertiary thermal conductivity was used to compute the temperatures for cases 1, 2, and 3. A variable Tertiary thermal conductivity was used to compute the temperatures for Case 4.

represent maximum values for the Tongue River Member of the Fort Union Formation in the study area.

Calculated temperatures for the Milo Fee 1 well are shown for the upper Tongue River Member (**Figure 13**) and the lower Tongue River Member (**Figure 14**). With 1,000 m of erosion, maximum temperature reached 41°C in the upper Tongue River Member and 49°C in the lower Tongue River Member. We also constructed temperature histories for the Mowry Shale in both wells similar to those shown in **Figure 12**, **Figure 13**, and **Figure 14**.

We calculated a final set of temperature curves for both the Cedar Draw 1 and Milo Fee 1 wells using variable Tertiary thermal conductivity to reflect sediment compaction. We used 1,000-meter erosional amounts in the calculations for both wells. Results for the basal and upper Tongue River Member during erosional events at 10 and 35 Ma are shown in **Figure 15** for the Milo Fee 1 well and in **Figure 16** for the Cedar Draw well.

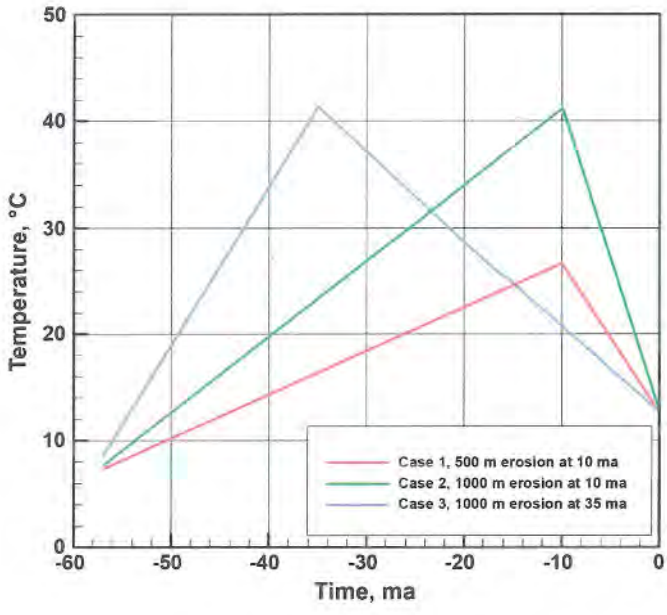

Figure 13. Time-temperature profile for the upper Tongue River Member of the Fort Union Formation at the Milo Fee 1 well in the study area. Case 1 assumes an erosional amount of 500 m for the most recent erosional event starting 10 Ma. Case 2 assumes an erosional amount of 1,000 m for the most recent erosional event starting 10 Ma. Case 3 assumes an erosional amount of 1,000 m for the most recent erosional event starting 35 Ma. A constant Tertiary thermal conductivity was used to compute the temperatures for all three cases.

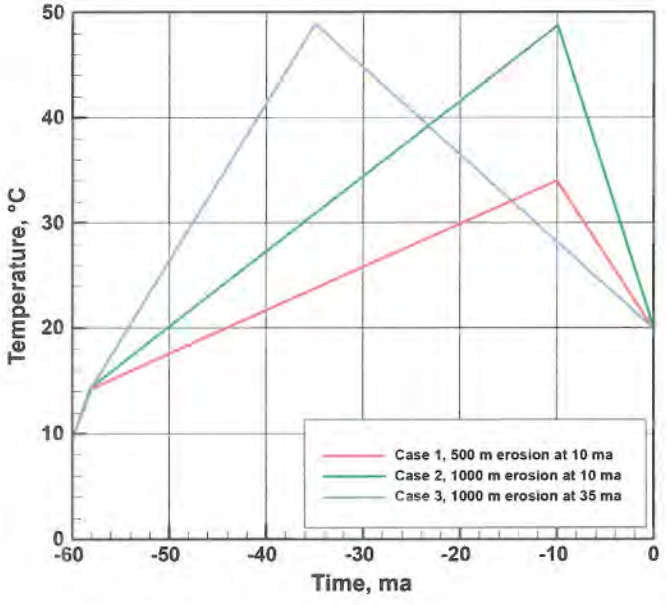

Figure 14. Time-temperature profile for the lower Tongue River Member of the Fort Union formation at the Milo Fee 1 well in the study area. Case 1 assumes an erosional amount of 500 m for the most recent erosional event starting at 10 Ma. Case 2 assumes an erosional amount of 1,000 m for most recent erosional event starting at 10 Ma. Case 3 assumes an erosional amount of 1,000 m for most recent erosional event starting at 35 Ma. A constant Tertiary thermal conductivity was used to compute the temperatures for all three cases.

Figure 15. Time-temperature profile for the upper and lower Tongue River Member of the Fort Union Formation at the Milo Fee 1 well in the study area. An erosional amount of 1,000 m was used for the most recent erosional event starting either 10 Ma or 35 Ma for all cases. A variable Tertiary thermal conductivity was used to compute the temperatures for all erosional scenarios.

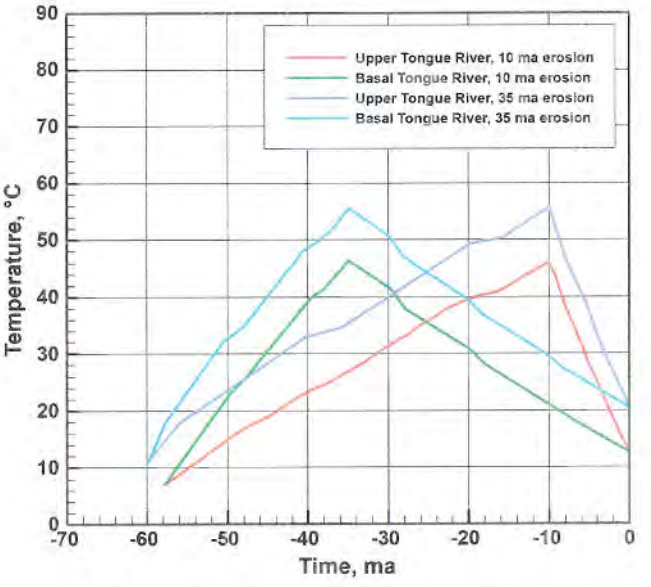

Figure 16. Time-temperature profile for the upper and lower Tongue River Member of the Fort Union Formation at the Cedar Draw 1 well in the study area. An erosional amount of 1,000 m was used for the most recent erosional event starting either 10 Ma or 35 Ma for all cases. A variable Tertiary thermal conductivity was used to compute the temperatures for all erosional scenarios. The temperature at maximum burial reached 65°C in the lower Tongue River Member at the Cedar Draw 1 well.

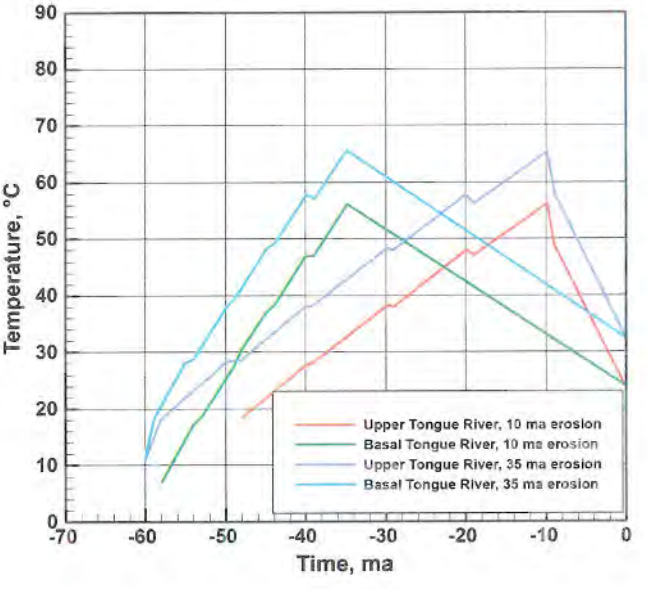

Maturation modeling

The maturation modeling techniques of Tissot and Welte (1978) were used to evaluate the maturation level of the stratigraphic section in the study area. In these techniques, activation energies and frequency factors for a specific type of kerogen are numerically integrated over the temperature history for the unit of interest. This calculation yields the percentage of kerogen that has been thermally altered or converted to hydrocarbons or organic acids. This percentage (representing reaction progress) ranges from 0.0 (no conversion) up to 1.0 (complete conversion), and has been termed the *transformation ratio* (the ratio of hydrocarbons generated to the genetic potential of a specific kerogen type). Tissot and Welte (1978) consider a transformation ratio of 0.4 to represent the threshold value for the kerogen to gas reaction. The threshold transformation ratio for the oil to gas reaction occurs at values less than 0.4.

For all burial cases in both wells, the transformation ratios for both Type II and Type III kerogen in the basal Tongue River Member were less than 0.1 (**Figure 17**). Only very small (trace) amounts of thermogenic gas could have been generated (0.0055 mg/g TOC) ac-

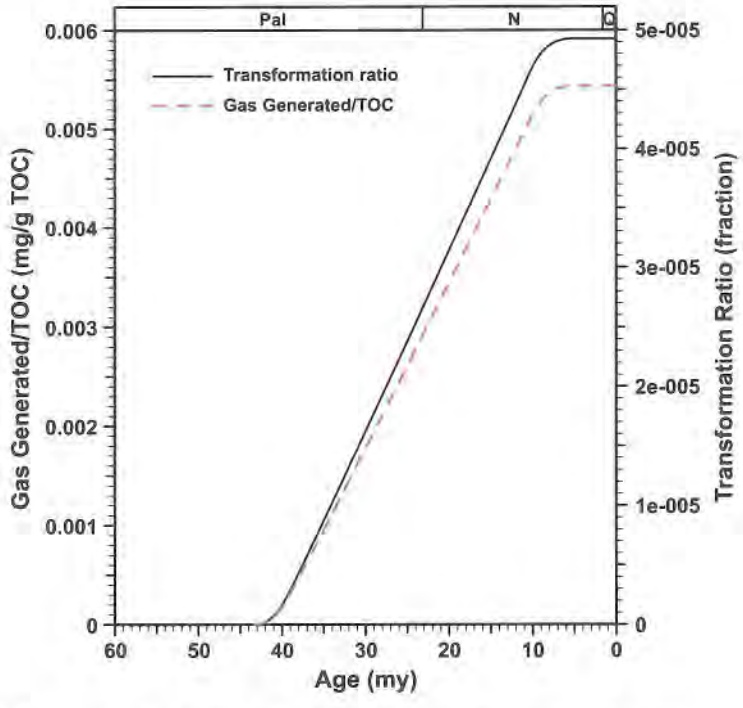

Figure 17. Plot of transformation ratio and gas generation versus time for the lower Tongue River Member coals at the Cedar Draw 1 well in the Powder River Basin, Wyoming. Only trace amounts of thermogenic gas were generated (0.0055 mg/g TOC) during maximum burial.

cording to the burial histories of the coal beds in the Tongue River Member. Therefore, we conclude that the Tongue River Member has not generated thermogenic gas.

For comparison purposes, we evaluated the transformation ratio for the Mowry Shale (the stratigraphic interval between the Muddy and Frontier formations as shown in **Figure 2**) in the Cedar Draw 1 well. **Figure 18** shows the results. The transformation ratio equals 1 at 47 Ma (indicating the reaction of kergogen to liquid hydrocarbon is complete). Therefore, the Mowry Shale is beyond the late generation stage (meaning that the kerogen to oil and gas reaction, and the oil to gas reaction, are both complete). **Figure 19** shows the potential amount of gas generation (mg) per gram of total organic carbon in the Mowry and Frontier formations that has occurred along the cross section shown in **Figure 2**. This value (500 mg/g TOC) is exceptionally high, and suggests that the Mowry Shale in the study area produced copious amounts of thermogenic gas in the Powder River Basin. This conclusion is supported by ^{13}C nuclear magnetic resonance (NMR) of the Mowry Shale samples, which shows a significant reduction of aliphatic functional groups with progressive burial (at 9,000 ft present-day depth, the aliphatic peak in the Mowry Shale NMR spectra is almost gone; see **Figure 18** in Surdam et al.,1997).

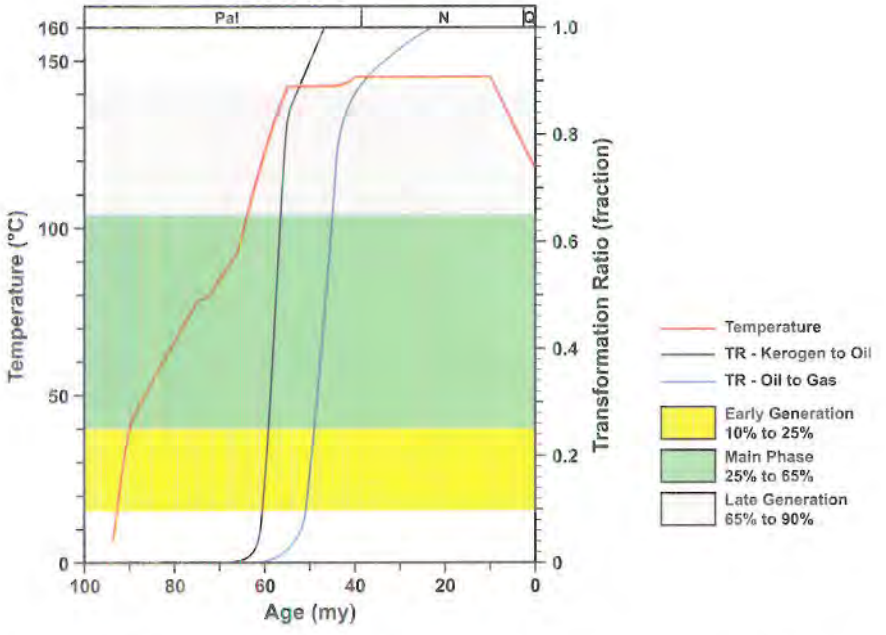

Figure 18. Time-temperature and time-transformation profiles for the upper Cretaceous Mowry Shale at the Cedar Draw 1 well. The Mowry Shale is beyond the late generation stage (the kerogen to oil and gas reaction and oil to gas reaction are both complete).

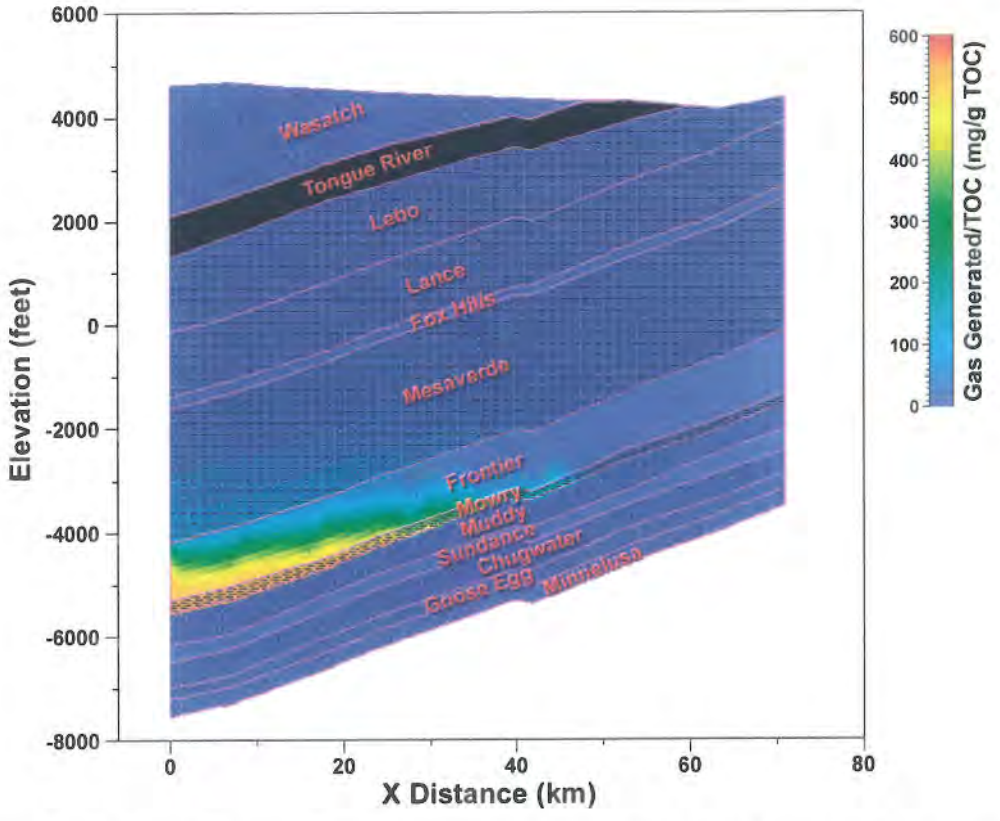

Figure 19. The thermal maturation cross section constructed for the stratigraphic section illustrated in Figure 1, showing the amount of gas (mg) generated per gram of total organic carbon in the Mowry and Frontier formations. This value (500 mg gas/g TOC) is exceptionally high and suggests that the Mowry Shale in the study area is a source of copious amounts of thermogenic gas.

Hydrous Pyrolysis

The experimental hydrous pyrolysis apparatus and the procedures used to simulate the thermal maturation of coals in the Tongue River Member are described in Winters et al. (1983). We ran all experiments isothermally at temperatures ranging from 260-360°C for 72 hours. We removed the products of pyrolysis after the reaction vessel cooled to room temperature (approximately 24 hours). We collected gas samples through a valve on the gauge head before opening the reaction vessels. Gas samples were stored for analysis in either glass or metal cylinders. The reaction vessels used were 1L Parr Instrument high-pressure thermometric vessels.

To collect fragments ranging from 0.5 to 2.0 mm in size, we ground and sieved the samples. A total of 120 grams of sample (coal) was combined with 120 grams of distilled water in a reaction vessel. To minimize damage to the steel reaction vessels, we used distilled water instead

of saline solution. To remove carbon dioxide gas, we boiled the distilled water before mixing it with the coal sample. We purged the mixture of sample and distilled water with pressurized helium gas after sealing the reaction vessel.

The reaction vessels were cleaned with distilled water and brushed with a soft bristle brush after each pyrolysis run. A film of graphite and amorphous carbon, which forms during the runs, was maintained on the inside of the vessels to prevent the steel from catalyzing the decarboxylation of mono- and di-functional acids formed during the experiment.

We derived kinetic parameters for hydrocarbon and organic acid generation by assuming first order rate kinetics using standard Arrhenius plots (Tissot and Espitalie, 1975). The methodology for analyzing hydrous pyrolysis data is described in detail in Lewan (1985). The basic equation used to calculate the rate constant from the experimental data was

$$-\ln k = \ln\{\ln[1/(1-x)]\}/\text{time}$$, where:

x is the weight fraction of hydrocarbon (normalized to maximum production), or the mole percent carboxylic acid generation; and

k is the reaction rate constant.

We can use the rate constant (k) in the Arrhenius equation ($k=Ae^{(-Ea/RT)}$) to calculate the activation energy (E_a) and pre-exponential factor (A) by plotting the log of the concentration of products (ln k) versus 1/temperature (1/T). The slope of the line derived by exponentially fitting the data points is equal to the activation energy divided by the Universal Gas Constant, and the y-intercept represents the pre-exponential factor.

Figure 20 shows the Arrhenius plot resulting from hydrous pyrolysis experiments using Tongue River Member coal samples from the Rawhide Mine in the Powder River Basin. We derived an activation energy (E_a) of 27.3 kcal and a pre-exponential factor (A) of $1.73x10^{18}$ for thermogenic liquid hydrocarbon generated from coal from this plot. We used the kinetics of the oil to gas reaction from Mackenzie and Quigley (1988) to calculate the oil to gas transformation ratio. **Figure 21** shows the Arrhenius plot for the generation of acetate from the Tongue River coal, as well as the data for the decarboxylation of acetate. For acetate generation, the activation energy is 24.6 kcal and the pre-exponential factor is $1.96x10^{16}$.

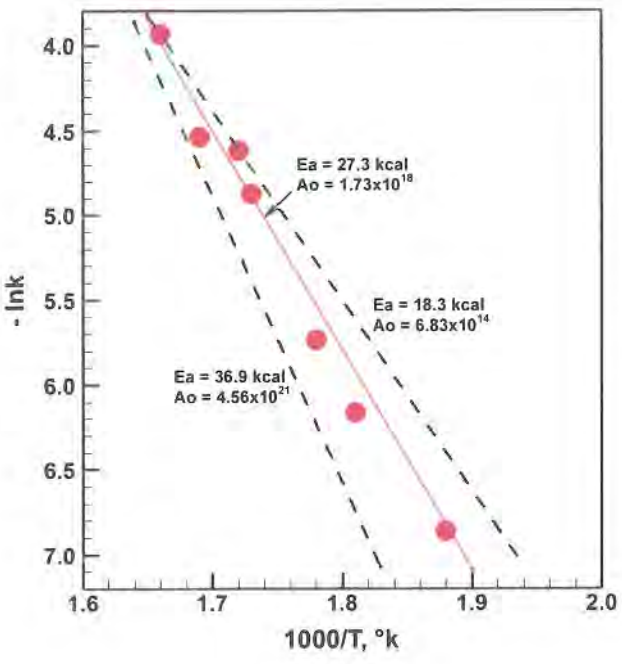

Figure 20. The Arrhenius plot derived from hydrous pyrolysis experiments for Tongue River Member coal samples from the Rawhide Mine in the Powder River Basin. The slope of a line derived by exponentially fitting the data points (a linear line on the plot) is equal to the activation energy divided by the Universal gas constant, and the y intercept represents the pre-exponential factor. An activation energy (E_a) of 27.3 kcal and a pre-exponential factor (A) of 1.73×10^{18} for thermogenic liquid hydrocarbon generated from coal can be derived from this plot.

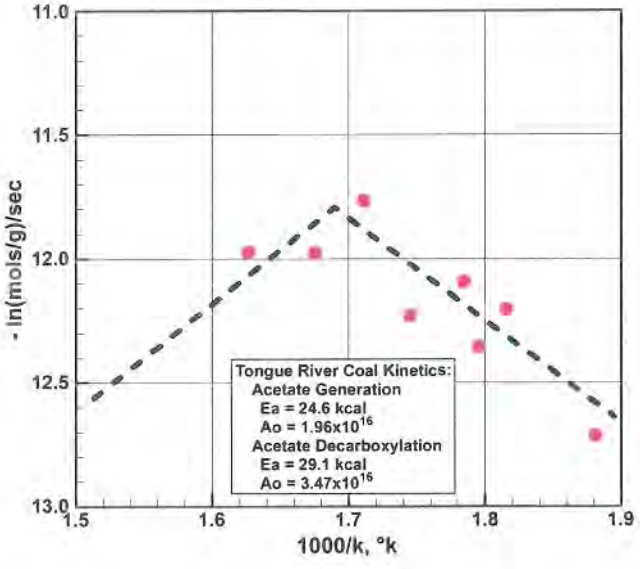

Figure 21. The Arrhenius plot resulting from hydrous pyrolysis experiments for Tongue River Member coal samples from the Rawhide Mine, showing the generation of acetate from the Tongue River Member coal, as well as data for the decarboxylation of the acetate. For acetate generation, the activation energy is 24.6 kcal and the pre-exponential factor is 1.96×10^{16}. For acetate decarboxylation, the activation energy is 29.1 kcal and the pre-exponential factor is 3.47×10^{16}.

Vitrinite Reflectance

Vitrinite reflectance measurements and organic chemistry analyses were performed on the Tongue River coal samples from the Rawhide Mine. Two samples were analyzed for vitrinite reflectance (R_0) by Geochem Laboratories in Houston; **Figure 22** and **Figure 23** show the results. Both samples show several different vitrinite populations. Because these samples were collected from a fresh mine face, there is no possibility of contamination by caving or from drilling mud. Therefore, a reasonable interpretation is that the vitrinite population with the higher reflectance values (R_0 = 0.6 to 1.2) indicates contamination by non-indigenous vitrinite at the time of coal deposition. For example, Permian and Cretaceous coals were undoubtedly exposed in the Tertiary drainage basin during deposition of the Tongue River Member coals. Transport and redeposition of vitrinite from these older coal beds during the deposition of the Tertiary coal beds may explain the R_0 values in the 0.6-1.2 range. In addition, material from the locally-exposed clinker beds could have contaminated the samples. If the higher, or more mature, vitrinite populations stemmed from contamination, then the indigenous R_0 value would range from 0.32 to 0.41. This range agrees with the coal rank reported by Law et al. (1991) for the Fort Union coal beds. Law reported that the rank of coal in the Fort Union varies from lignite to subbituminous B, which is equivalent to a range in mean random vitrinite reflectance of 0.28-0.45.

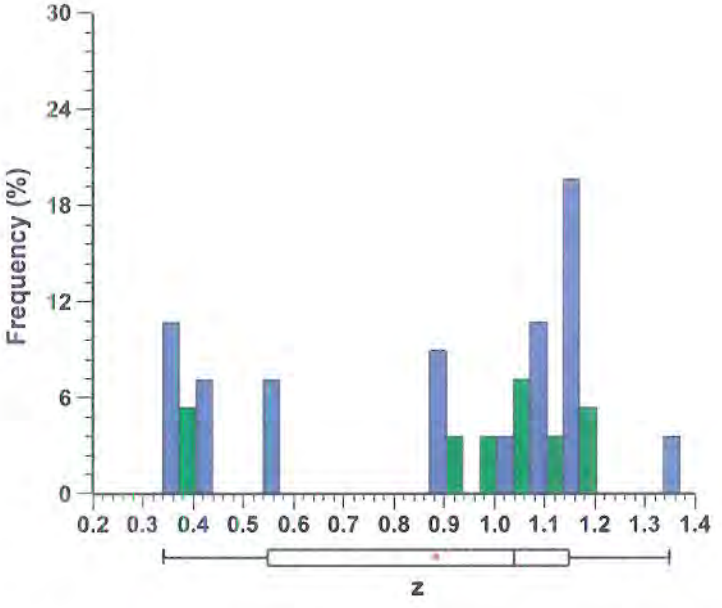

Figure 22. A histogram of vitrinite reflectance of the Tongue River Member coals from the Rawhide Mine, Powder River Basin, Wyoming.

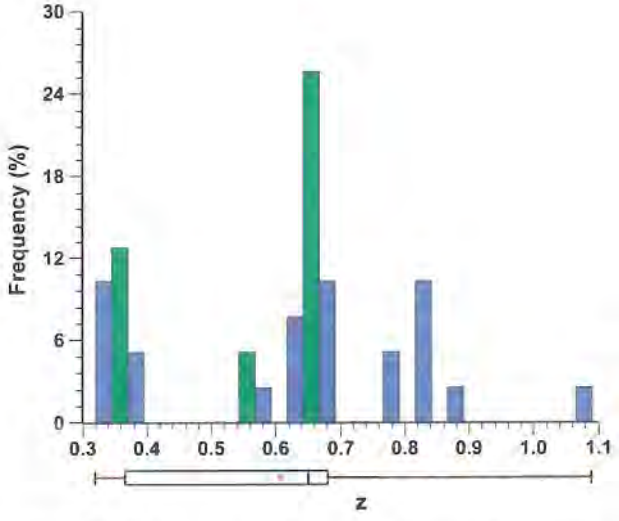

Figure 23. A histogram of vitrinite reflectance of the Tongue River Member coals from the Rawhide Mine, Powder River Basin, Wyoming.

Table 3 shows the organic geochemistry of the Tongue River coal samples from the Rawhide Mine. The measured production index (PI) of 0.03 shown in **Table 3** suggests that the coal is immature. Typically, entrance to the liquid hydrocarbon generation window occurs at a PI of 0.1. The PI value of 0.03 agrees with the R_0 assignment (0.41) made for the indigenous vitrinite reflectance value. Lastly, a hydrogen index (HI) of 235 suggests that the coal retains most of its potential as a gas source, and a genetic potential (GP) of 157 suggests that, with more elevated thermal exposure, the coal could be a prolific source of thermogenic gas.

As an additional check on the validity of assigning a R_0 value of 0.41 to the indigenous vitrinite reflectance, we used a kinetic model to calculate R_0 using the derived temperature histories for the Tongue River Member coal. The vitrinite kinetic values used in this model were derived from Frontier Formation samples collected in the Bighorn Basin (Angelos et al. 1988). Results of this calculation are shown in **Table 4**. Depending on stratigraphic positions in the unit and parameters used to construct the thermal histories, modeled values of R_0 range from 0.36 to 0.45 for the Tongue River Member. These modeled R_0 values support the selection of 0.41 as the R_0 of the indigenous vitrinite for the coal samples analyzed for vitrinite reflectance.

Table 3. Geochemical parameters for the Tongue River coal.

Inorganic Carbon (weight percent)	0.02
Organic Carbon (weight percent)	64.65
Nitrogen (weight percent)	0.84
Hydrogen (weight percent)	4.81
S_1 (mg HC/g TOC)	4.79
S_2 (mg HC/g TOC)	152
T_{max} (°C)	462
P.I.	0.03
H.I.	235
G.P.	157

Table 4. Calculated vitrinite reflectance (R_0) values.

Sedimentary Unit	Milo Well		Cedar Draw Well	
	1,000 m erosion		*1,000 m erosion*	
	at 10 ma[1]	at 35 ma[1]	at 35 ma[1]	at 35 ma[2]
Upper Tongue River	0.36	0.37	0.40	0.40
Basal Tongue River	0.40	0.40	0.45	0.45
Basal Mowry	1.15	1.17	1.44	1.51

[1] *Calculated assuming constant layer thermal conductivities as shown in Table 2 and discussed in text.*

[2] *Calculated assuming a porosity-dependent thermal conductivity for the Tertiary section.*

Biogenic Gas and Pathways

Though the coal beds of the Tongue River Member have generated no thermogenic gas, they have huge potential for the generation of biogenic gas. Biogenic gas, which accounts for 20% of all known natural gas resources (Rice and Claypool, 1981), is defined as gas generated in the methanic diagenetic (methanogenesis) zone (Berner, 1981; Maynard, 1982), so named because of the dominant role played by methanogenic microorganisms in sediments and fluids of the methane biogeochemical zone (Claypool and Kaplan, 1974), and because a principle product of the zone is methane (CH_4). Biogenic methane production is known to occur over a temperature range of 0°C to 75°C (Bushwell and Mueller, 1952; Zeikus and Winfrey, 1976). In general, biogenic methane is generated in significant amounts between the base of the sulfate reduction zone (commonly at depths of a few meters) to depths of approximately 1,000 m (Price and Claypool, 1981). Biogenic methane is identified in ancient and modern sediments on the basis of molecular composition (C1/C1-C5 = 1) and isotopic signature ($\delta^{13}C$ < -50%; Gautier, 1985). **Figure 24** shows effects of mixing thermal and bacterial gases with different isotopic values.

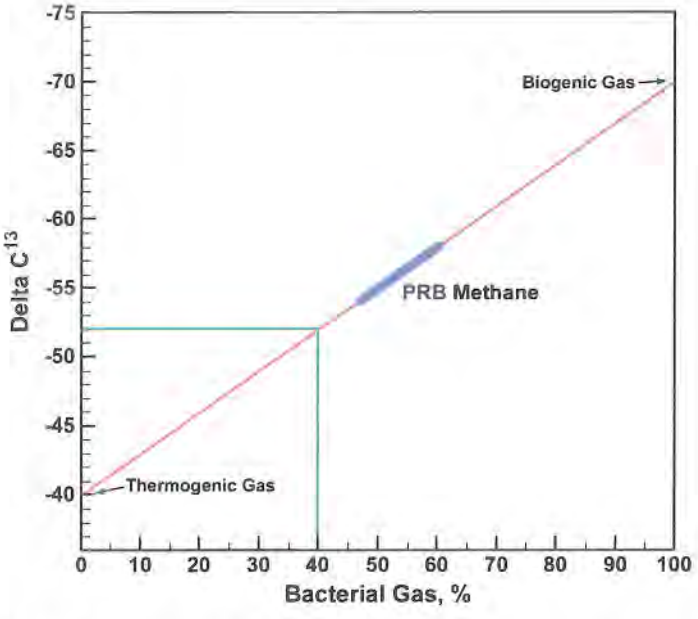

Figure 24. The range of the carbon isotopic values resulting from the mixing of thermal and bacterial gases (Barker 1987). The Tongue River Member coal and adjacent sandstone are isotopically light ($\delta^{13}C$ value ranges from -54% to -58%: thick solid blue line in diagram), indicating that the coalbed gas in the Tongue River Member is a mixture of thermogenic and biogenic gas.

As can be seen from **Figure 12** through **Figure 16**, regardless of the burial-thermal scenario chosen, both the top and bottom of the Tongue River Member containing the coal beds of interest have been within the thermal interval of methane diagenesis (zone of methanogenesis) for the last 60 million years (at temperatures less than 75°C). The exceptionally high organic content of the coal beds and the long residency time in the zone of methanic diagenesis ensures that the coal beds in the Tongue River Member have generated copious quantities of biogenic methane.

Once the isotopic signature of the methane is known, **Figure 24** can be used to determine the potential for mixing thermogenic and biogenic methane. Law et al. (1991) reported that methane samples from the Tongue River Member coal and adjacent sandstone are isotopically light ($\delta^{13}C$ value ranges from -54% to -58%), and depleted in deuterium (δDI value ranges from -307% to -345%). Plotting these values on **Figure 24** reveals that the coalbed gas in the Tongue River Member is a mixture of thermogenic and biogenic gas. The thermogenic gas probably migrated from the deeper section, especially from units like the Mowry Shale in the Powder River Basin.

Two pathways have been identified for the generation of biogenic gas in the zone of methanogenesis: carbon dioxide reduction and methyl-type fermentation (Schell, 1980; Whiticar et al., 1984). Carbonate reduction occurs primarily in marine water containing sulfate, while acetate fermentation occurs in environments consisting of relatively fresh water (Whiticar et al., 1984; Scott, 1999). The Tertiary Tongue River Member coals of the Fort Union Formation in the PRB were deposited in a fresh water, low-sulfate, paludal/lacustrine environment (Flores and Hanley, 1984; Ayers, 1986). Whiticar et al. (1984) constructed a natural gas genetic classification diagram using $\delta^{13}C$ and δD of methane (**Figure 25**). From this diagram, the biogenic methane significantly depleted in deuterium resulting in acetate-type fermentation can be distinguished from gas produced by carbonate reduction. The $\delta^{13}C$ and δD of the CBNG from the PRB clearly fall in the field of acetate-type fermentation, but lie near the transitional field between fermentation and thermogenic gas (Rice, 1993). Based on these observations, we assume that the biogenic component of the CBNG in the coals of the Tongue River Member in the PRB results primarily from acetate fermentation, not carbon dioxide reduction. We conclude that the biogenic natural gas resulting from methanogenesis of the coals took place during progressive burial and not after uplift and exposure to relatively recent meteoric water. Therefore, the key to understanding the origin of the biogenic natural gas in the Tongue River Member coals in the PRB is determining the timing of the availability of short-chain carboxylic acids such as acetic acid and acetate anions.

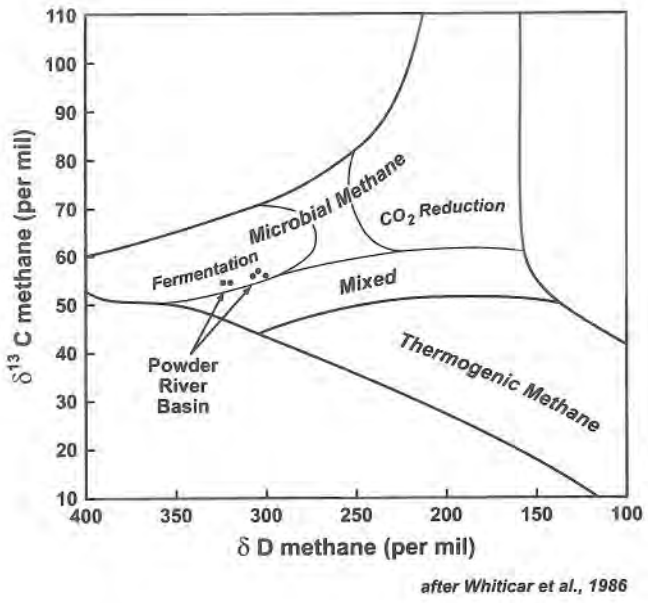

Figure 25. Natural gas genetic classification diagram using $\delta^{13}C$ and δD of methane modified from Whiticar et al. (1986). Isotopically, biogenic methane resulting from acetate-type fermentation can be distinguished from biogenic methane resulting from CO_2 reduction. Biogenic and thermogenic methane can also be distinguished on the diagram. Powder River Basin Tertiary coal sample compositions are from Rice (1993).

Acetate Generation

In the zone of methanogenesis, bacteria reduce their feedstock to methane and carbon dioxide. Short-chained carboxylic acid anions such as acetate provide an ideal food source for methanic bacteria (acetate fermentation: $CH_3COO^- + H^+ \rightarrow CH_4 + CO_2$). The acetate fermentation involves the reduction (decomposition) of acetate by methanogenic bacteria to produce methane. Experimental observations demonstrate that the process of methanogenesis (fermentation) by bacteria is strongly influenced (initiated and/or greatly accelerated) by the presence of acetate. The availability of useable food, such as acetate, for the bacteria determines the extent to which the process of methanogenesis can proceed. Therefore, the zone of methanogenesis during the burial of a coal bed can be approximated by the availability of acetate.

Using the kinetic parameters derived from hydrous pyrolysis for the chemical reaction forming acetate from coal, it is possible to determine the distribution of acetate in the coal as a function of burial. This determination is accomplished by numerically integrating the acetate kinetic parameters over the calculated temperature histories of the Tongue River Member using a first-order Arrhenius equation (technique modified from Tissot and Welte, 1978). **Figure 26** and **Figure 27** show results of this modeling (acetate generation reaction). **Figure 26** shows the acetate generation curve of the upper and lower Tongue River Member from the Milo Fee well assuming variable Tertiary thermal conductivity and erosional events occurring either 35 Ma or 10 Ma. **Figure 27** shows the acetate generation curve of the upper and lower Tongue River Member from the Cedar Draw well assuming variable Tertiary thermal

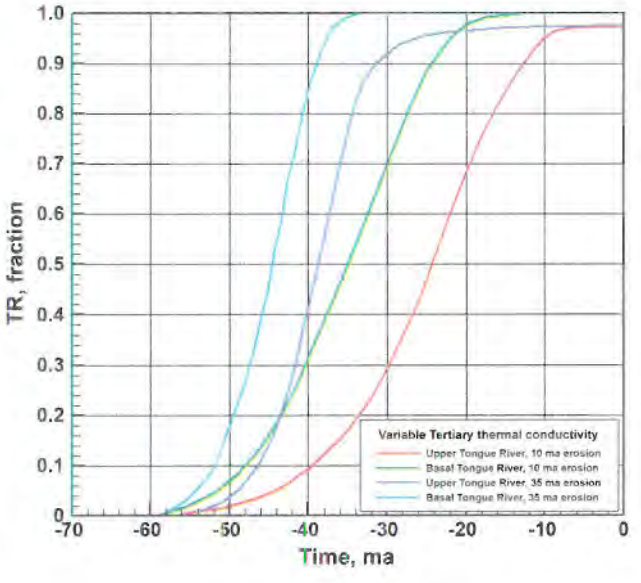

Figure 26. The transformation curves for acetate generation in the upper and lower Tongue River Member in the Milo Fee 1 well. The time-temperature reconstruction is based on variable Tertiary thermal conductivity and an erosional amount of 1,000 m at either 35 Ma or 10 Ma.

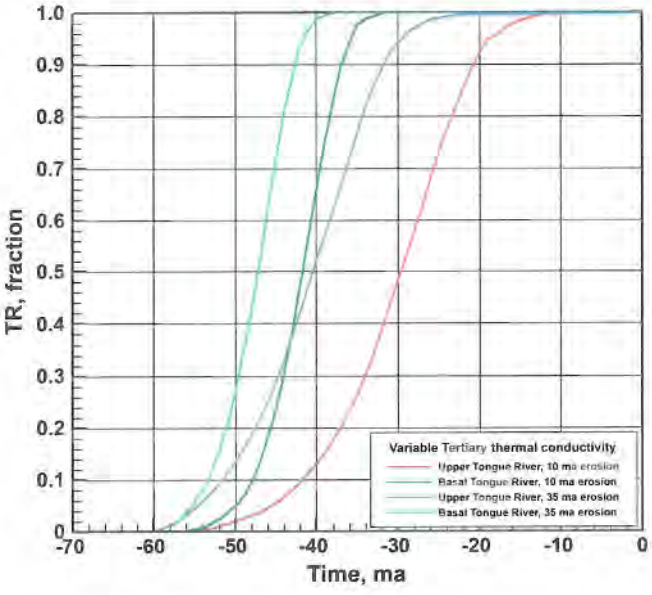

Figure 27. The transformation curves for acetate generation in the upper and lower Tongue River Member in the Cedar Draw 1 well. The time-temperature reconstruction is based on variable Tertiary thermal conductivity and an erosional amount of 1,000 m at either 35 Ma or 10 Ma.

conductivity and erosional events occurring at either 35 Ma or 10 Ma. The temperature histories used in this calculation are shown in **Figure 15** and **Figure 16**. The acetate decarboxylation transformation ratio is 0.1 for the Milo Fee well, and smaller for the Cedar Draw 1 well (**Figure 28**). These results suggest that for Tongue River Member coals in both wells, acetate generation is complete and only approximately 10% of the acetate has been thermally decarboxylated (destroyed) along the cross section shown in **Figure 1** and **Figure 2**.

As can be seen from **Figure 26** and **Figure 27**, the coals in the Tongue River Member exhausted their acetate-generation capacity by 10 Ma. By using **Figure 26** and **Figure 27** along with the burial histories shown in **Figure 5**, **Figure 7**, **Figure 9**, and **Figure 10**, a range of depths can represent the beginning of rapid acetate generation (defined here as a transformation ratio of 0.1) and the completion of rapid acetate generation (defined here as a transformation ratio of 0.9). The times, temperatures, and depths for acetate generation transformation ratios of 0.1 to 0.9 are listed in **Table 5**. As shown in **Table 5**, the beginning of acetate generation generally occurs at burial depths of approximately 500 m, and completion of rapid acetate generation occurs at burial depths of approximately 1,000 m.

In addition to allowing us to calculate kinetic values for acetate generation and decarboxylation, the hydrous pyrolysis experiments suggest that the coals in the Tongue River Member are capable of generating at least 0.133 moles (7.8 grams) of acetate per kilogram of coal.

Solid-state ^{13}C Nuclear Magnetic Resonance (NMR) analysis can provide direct insight into the structural changes taking place in kerogen within coal beds during progressive burial

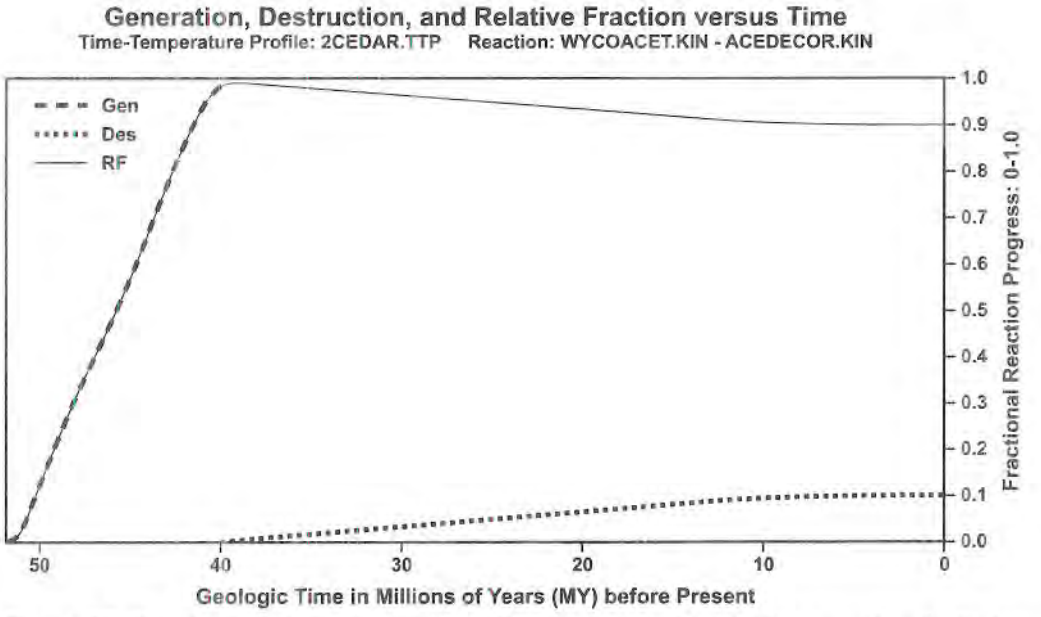

Figure 28. Plot of the acetate generation, thermal destruction, and relative fraction versus time for the lower Tongue River Member in the Powder River Basin, Wyoming. The results shown here were computed using in-house thermal modeling software. The kinetic parameter for this modeling was derived from the hydrous pyrolysis data shown in Figure 21.

(Miknis et. al., 1982; Garcia-Gonzalez and Surdam, 1995). In near-surface coal samples, the kerogen typically contains aliphatic and aromatic functional groups, as well as significant amounts of carbonylic functional groups. The carbonylic functional groups are oxygen-bearing and are among the first functional groups cleaved from kerogen during early burial. The production of oxygen-bearing functional groups (carboxylic acid and acid anions) is a natural product of early diagenesis of coals. Solid-state ^{13}C NMR analyses of suites of coal samples taken from near-surface depths (~ 200 ft) to depths as great as 10,500 ft demonstrate that the oxygen-bearing functional groups have been greatly reduced at burial depths of approximately 3,000 ft, and are nearly absent from the kerogen in the coals at burial depths of approximately 5,000 ft (Surdam et al., 1989). These observations demonstrate that the ability of kerogen to serve as a feedstock for methanogenic bacteria is substantially reduced once coal beds are buried to depths below 4,000 ft.

Yin et al. (1993) used NMR techniques to show that the at-surface, immature brown coals of Australia's Gippsland Basin have vitrinite reflectance values (R_0) of 0.21-0.23 and contain 5% or more oxygen-bearing functional groups (carboxylic acid and acid anion precursors). These oxygen-bearing functional groups are gone in the same coals buried at depths of 4,600 feet (R_0 ~ 0.45, **Figure 29**). These observations further support the suggestions that: 1) im-

mature kerogen in coals contains copius quantities of potential feedstock for methanogenic bacteria in the form of oxygen-bearing functional groups; 2) this feedstock becomes available in the form of short-chained carboxylic acids and acid anions during early burial and shallow diagenesis; 3) this food source disappears from the coal at burial depths of approximately 4,500 feet; and 4) both bacterial methanogenic activity and thermal decarboxylation of the short-chained carboxylic acids and acid anions generates methane.

Table 5. Acetate generation reaction transformation ratio (TR), time, temperature, and burial depth of the Tongue River coal in the Milo and Cedar Draw wells.

Milo Well, 10 Ma erosional event				
	TR	*Time (Ma)*	*Temperature (°C)*	*Depth (m)*
Upper Tongue River	0.1	39	24	386
	0.9	13	44	961
Basal Tongue River	0.1	48	26	431
	0.9	24	46	1,013
Milo Well, 35 Ma erosional event				
	TR	*Time (Ma)*	*Temperature (°C)*	*Depth (m)*
Upper Tongue River	0.1	46	29	499
	0.9	31	43	934
Basal Tongue River	0.1	52	29	499
	0.9	39	50	1,117
Cedar Draw Well, 10 Ma erosional event				
	TR	*Time (Ma)*	*Temperature (°C)*	*Depth (m)*
Upper Tongue River	0.1	42	25	443
	0.9	21	47	1,087
Basal Tongue River	0.1	51	27	492
	0.9	32	46	1,059
Cedar Draw Well, 35 Ma erosional event				
	TR	*Time (Ma)*	*Temperature (°C)*	*Depth (m)*
Upper Tongue River	0.1	48	30	566
	0.9	37	52	1,222
Basal Tongue River	0.1	53	31	591
	0.88	51	51	1,195

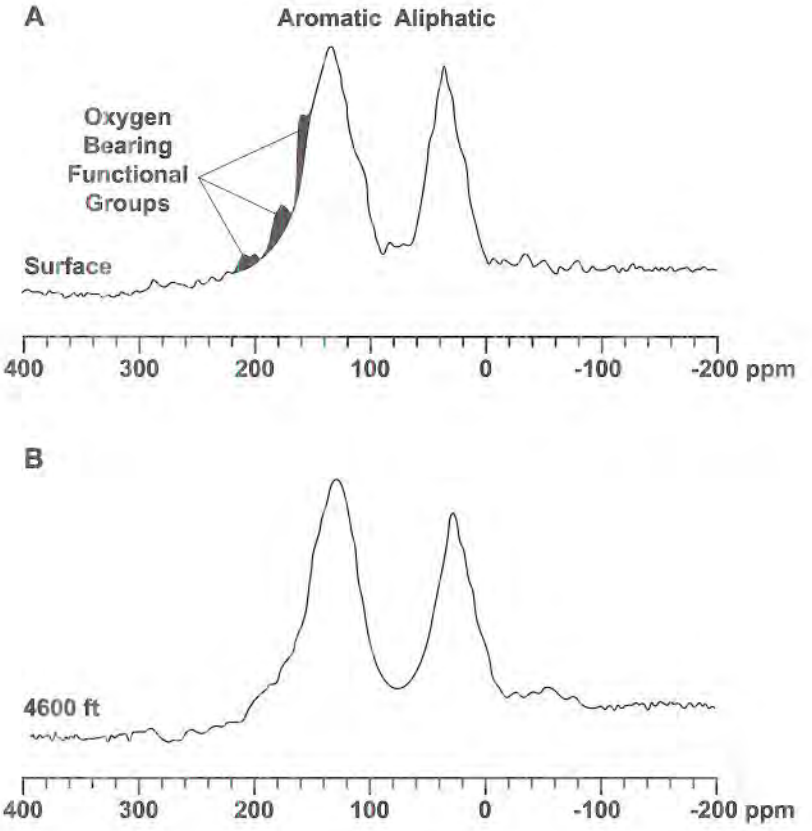

Figure 29. Changes in the NMR spectrum from at-surface brown coal sample (**A**, top; R_o = 0.21-0.23) to a brown coal sample (**B**, bottom; $R_o \approx 0.45$) at a depth of 4,600 feet. Both samples are from the Gippsland Basin of Australia. Oxygen-bearing functional groups are shown in black; the aromatic functional groups are represented by the large peak on the left, and the aliphatic functional groups are represented by the large peak on the right.

Summary

This report describes the methodology and data used to construct burial, temperature, and maturation histories for the Paleocene Tongue River Member of the Fort Union Formation in the northeastern Powder River Basin of Wyoming. In order to determine the potential for thermogenic and biogenic gas generation from kerogen contained in the coals of the Tongue River Member, we reconstructed burial, temperature, and erosional histories for the units of interest. More than 50 wells in the Powder River Basin were used to determine erosional amounts. Assuming 180 µs/ft for the original surface transit time, and given the data presented in **Table 1**, we estimate that a maximum of 1,000 m (3,280 ft) of erosion has occurred in the area west of Gillette, Wyoming. The maximum burial depth of the basal Tongue River Member is 1,900 m (6,230 ft) at Cedar Draw 1 well. With variable Tertiary thermal conductivity and 1,000 m of erosion, the temperature at maximum burial reached 62°C in the basal Tongue River Member at the Cedar Draw well. The maximum temperature reached 41°C in the upper Tongue River Member and 49°C in the lower Tongue River Member at the Milo Fee 1 well.

We used the maturation modeling techniques of Tissot and Welte (1980) to determine the thermal maturation levels of the Tongue River Member coals. The kinetic values used to evaluate the hydrocarbon maturation history of the Tongue River Member were taken from Tissot and Welte (1978) for Type II and Type III kerogens, and were validated using hydrous pyrolysis experiments. From hydrous pyrolysis experiments, we derived an activation energy (E_a) of 27.3 kcal and a pre-exponential factor (A) of 1.73×10^{18} for thermogenic liquid hydrocarbon generated from coal. In addition, we determined kinetic parameters for the reaction of coal to acetate using the hydrous pyrolysis technique. For acetate generation, the activation energy is 24.6 kcal and the pre-exponential factor is 1.96×10^{16}. Using both published and experimentally derived kinetics and constructed temperature histories, we modeled and evaluated the conversion of kerogen in coals to both hydrocarbons and acetate (i.e., short-chained carboxylic acid). For all burial scenarios in both wells, the transformation ratios for both Type II and Type III kerogen in the basal Tongue River Member is less than 0.1. Only trace amounts of thermogenic gas could have been generated (0.0055 mg/g TOC) from the coal beds. Therefore, we suggest that the coals in the Tongue River Member have not generated significant amounts of thermogenic gas.

The coals in the Tongue River Member generated all potential acetate by approximately 10 Ma. Rapid acetate generation generally begins at burial depths of approximately 500 meters and ends at burial depths of approximately 1,000 meters. In addition to allowing us to calculate the kinetic values for acetate generation and decarboxylation, the hydrous pyrolysis experiments suggest that the coals in the Tongue River Member are capable of generating at least 0.133 moles (7.8 grams) of acetate per kilogram of coal.

The Fort Union coal reserves in the PRB are estimated at 1 trillion tons. Therefore, methanogenesis in the Fort Union coals could generate $1.21 \cdot 10^{14}$ moles of methane (0.133 moles per kilogram of coal), or $1.936 \cdot 10^{12}$ kg of methane. This is equal to 95 TCF of the methane

generated in the Fort Union coal by fermentation. If the carbon dioxide reduction is taken into consideration, this number could be much larger.

Conclusion

The coal beds in the Paleocene Tongue River Member of the Fort Union formation are not the source of thermogenic methane in the coals located near Gillette, Wyoming. However, the Tongue River Member coal beds did produce copious quantities of biogenic methane. Isotopic characteristics of the coalbed natural gas in the Tongue River Member demonstrate that the gas is a mixture of thermogenic and biogenic gas. The biogenic gas present in the coals resulted from methanogenesis which occurred 50 to 10 Ma, during which time a huge quantity of short-chained carboxylic acids and acid anions (a favored feedstock for bacteria in the zone of methanogenesis) was available to the bacteria. According to this study, the Tongue River Member coal beds currently have little capacity to generate additional acetate. Any acetate presently available in the coals for methanogenesis was generated millions of years ago, but was not used by the methanogenic bacteria.

The thermogenic gas in the coals originated in underlying organic-rich rocks in the deeper Cretaceous section, such as those of the Frontier Formation or Mowry Shale. In brief, the natural gas produced from coals in the Tongue River Member of the Fort Union Formation in the Powder River Basin is a mixture of biogenic and thermogenic gases. The biogenic gas is generated and stored in-situ as a result of methanogenesis, while the thermogenic gas migrated into the Paleocene coal beds from deeper organic-rich rocks.

Acknowledgements

The authors wish to thank Steve Boese of the Department of Geology and Geophysics at the University of Wyoming for performing the hydrous pyrolysis experiments used in this research. Platte River Associates provided the BasinMod software used in part of the study, and their valuable assistance is acknowledged. Nick Jones and other colleagues at the Wyoming State Geological Survey contributed to our understanding of the distribution of coal beds in the Tongue River Member of the Fort Union Formation. We also gratefully acknowledge the graphic assistance provided by Allory Deiss and the editorial assistance provided by Meg Ewald, both of the Wyoming State Geological Survey.

REFERENCES

Angelos, C.P., H.P. Heasler, and R.C. Surdam, 1988, Quantitative prediction of vitrinite reflectance applied to geologic thermal histories: Submitted to American Association of Petroleum Geologist's Bulletin.

Ayers Jr., W.B., 1986, Lacustrine and fluvial-deltaic depositional systems, Fort Union Formation (Paleocene), Powder River Basin, Wyoming and Montana: AAPG Bulletin, v. 70, no. 11, p. 1651-1673.

Baldwin, B., and C.O. Butler, 1985, Compaction curves: American Association of Petroleum Geologists Bulletin, v.69, p. 622-626.

Barker, C., 1987, Development of abnormal and subnormal pressures in reservoirs containing bacterially generated gas: American Association of Petroleum Geologists Bulletin, v. 71, no. ii, p. 1404-1413.

Berner, R.A., 1981, A new geochemical classification of sedimentary environments: Journal of Sedimentary Petrology, v. 51, p. 359-365.

Buelow, K.L., H.P. Heasler, and B.S. Hinckley, 1986, Geothermal resources of the southern Powder River Basin, Wyoming: Geological Survey of Wyoming, Report of Investigations No. 36, 32 p.

Bushwell, A.M., and H.R. Mueller, 1952, Mechanisms of methane fermentation: Ind. Eng. Chemistry, v. 44, p. 550-552.

Claypool, G.E., and I.R. Kaplan, 1974, The origin and distribution of methane in marine sediments, in I.R. Kaplan, ed., Natural Gases in Marine Sediments: New York, Plenum Press, p. 99-139.

Flores, R.M., and Hanley, J.H., 1984, Anastomosed and associated coal-bearing fluvial deposits, Upper Tongue River Member, Paleocene Fort Union Formation, northern Powder River Basin, Wyoming, U.S.A., *in* Rahmani, R.A., and Flores, R.M. (eds.), Sedimentology of coal and coal-bearing sequences: International Association of Sedimentologists Special Publication 7, p. 85-103.

Garcia-Gonzalez, M., and Surdam, R. C., 1995, Hydrocarbon generation potential and expulsion efficiency in shales and coals, example from the Washakie Basin, Wyoming: Wyoming Geological Association 1995 Field Guidebook, p. 225-268.

Gautier, D.L., 1985, Relationship of organic matter and mineral diagenesis: Society of Economic Paleontologists and Mineralogists Lecture Notes, Short Course No. 17, SEPM, p. 6-72.

Hunt, J.M., 1979, Petroleum Geochemistry and Geology: Freeman, San Francisco, 617 p.

Law, Ben. E., Rice, Dudley D., and Flores, Romeo M. 1991, Coalbed gas accumulations in the Paleocene Fort Union Formation, Powder River Basin, Wyoming: in Rocky Mountain Association of Geologists Special Publication Coalbed Methane, p. 179-190.

Lewan, M.D., 1985, Evaluation of petroleum generation by hydrous pyrolysis experimentation: Philosophical Transactions of the Royal Society of London, Set. A, p. 123-134.

Love, J.D., 1960, Cenozoic sedimentation and crustal movement in Wyoming: American Journal of Science, v. 258 A, p. 204-214.

Love, J.D., 1970, Cenozoic geology of the Granite Mountains area, central Wyoming: United States Geological Survey Professional Paper 495-C, 154 p.

Mackenzie, A. S., and T. M. Quigley, 1988, Principles of geological prospect appraisal: American Association of Petroleum Geologists Bulletin, v. 72, p. 399-415.

Mackin, J.H. 1937, Erosional history of the Bighorn Basin, Wyoming: Geological Society of America Bulletin, v. 48, p. 813-893.

Magara, K., 1976, Thickness of removed sedimentary rocks, paleopore pressure and paleotemperature, southwestern part of western Canada Basin: American Association of Petroleum Geologist's Bulletin, v. 60. p. 554-565.

McCulloh, T.H., S.M. Cashman, and R.J. Stewart, 1978, Diagenetic baselines for interpretive reconstructions of maximum burial depths and paleotemperatures in clastic sedimentary rocks, *in* D.F. Oltz, ed., SEPM Symposium in Geochemistry: Low temperature metamorphism of kerogen and clay minerals, October 5, Los Angeles, California, p. 18-45.

Miknic, F. P., Smith, J. W., Maughan, E. K., and Maciel, G. E., 1982, Nulear magnetic resonance, a technique for direct nondestructive evaluation of source-rock potential: American Association of Petroleum Geologists Bulletin, v. 66, p. 1396-1401.

Mynard, J.B., 1978, Extension of Berner's "new classification of sedimentary environments" to ancient sediments: Journal of Sedimentary Petrology, v. 52, p. 1325-1331.

Rice, D.D., 1993, Composition and origins of coalbed gas, *in* Law, B. E., and Rice, D.D. (eds.). Hydrocarbons from Coal: American Association of Petroleum Geologists Studies in Geology No. 38, p. 159-184.

Rice, D.D., and G.E. Claypool, 1981, Generation, accumulation, and resource potential of biogenic gas: American Association of Petroleum Geologists Bulletin, v. 67, p. 5-25.

Rocky Mountain Association of Geologists, 1972, Geological Atlas of Rocky Mountain Region: published by RMAG, Denver, 331 p.

Schoell, M., 1980, The hydrogen and carbon isotopic composition of methane from natural gases of various origins: Geochemica et Cosmochemica Acta, v. 44, p. 649-661.

Scholle, P.A., 1977, Data summary and petroleum potential, in P.A. Scholle, ed., Geologic studies on the COST No. B2 well, United States Mid-Atlantic outer continental area: United States Geological Survey Circular 750, p. 8-14.

Sclater, J.G., and P.A.F. Christie, 1980, Continental stretching: an explanation of the post-mid-Cretaceous subsidence of the central North Sea Basin: Journal of Geophysical Research, v. 85, p. 3711-3739.

Scott, A. R., 1999, Improving coal gas recovery with microbially enhanced coalbed methane, in Mostalerz, M., Glikson, M., and Golding, S.D. (eds.), Coalbed Methane: Scientific, Environmental and Economic Evolution, Kluwer Academic Publishers, p. 89-110.

Steckler, M.S., and A.B. Watts, 1978, Subsidence of the Atlantic-type continental margin off New York: Earth and Planetary Letters, v. 41, p. 1-13.

Sundell, K.A., 1985, The Castle Rock chaos: a gigantic Eocene landslide-debris flow within the southwestern Absaroka Range, Wyoming: Unpublished Ph.D. dissertation, University of California at Santa Barbara, 236 p.

Surdam, R. C., Crossey, L. J., Hagen, E. S., and Heasler, H. P., 1989, Organic-inorganic interactions and sandstone diagenesis: American Association of Petroleum Geologists Bulletin, v. 73, p. 1-32.

Surdam, R. C., Z. S. Jiao, and H. P. Heasler, 1997, Anomalously pressured gas compartments in the Cretaceous rocks of the Laramide basins of Wyoming: a new class of hydrocarbon accumulation: in Surdam, R. C., ed., Seals, Traps, and the Petroleum System, American Association Petroleum of Geologists Memoir 67, p. 199-222.

Tissot, B.P., and J. Espitalie, 1975, L'evolution thermique de la matiere organique des sediments; applications d'une simulation mathematique potentiel petrolier des basins sedimentaires et reconstitution de l'histoire thermique de sediments: Revue de l'Institut Francais du Petrole, v. 30, p. 743-777.

Tissot, B.P , and D.H. Welte, 1984, Petroleum Formation and Occurrence, 2nd edition: New York, Springer-Verlag, 699 p.

Van Houten, F. B. 1952, Sedimentary record of Cenozoic orogenic and erosional events, Bighorn basin, Wyoming: Wyoming Geological Association 7th Annual Field Conference Guidebook, p. 74-79.

Waples, D.W., 1980, Time and temperature in petroleum formation: application of Lopatin's methods to petroleum exploration: American Association of Petroleum Geologist's Bulletin, v. 64, p. 916-926.

Whiticar, M.J., Faber, E., and Schoell, M., 1986, Biogenic methane formation in marine and freshwater environments – CO_2 reduction vs. acetate fermentation, isotopic evidence: Geochemica et Cosmochemica Acta, v. 50, no. 5, p. 693-709.

Winters, J.C., J.A. Williams, and M.D. Lewan, 1983, A laboratory study of petroleum generation by hydrous pyrolysis, *in* M. Bjoroy, C. Albrecht, C. Cornford, K. de Groot, G. Eglinton, E. Galimov, D. Leythaeuser, R. Pelet, J. Rullkotter, and G. Speers, eds., Advances in Organic Geochemistry 1981: Chichester, .England, John Wiley, p. 524-533.

Yin, P., R. C. Surdam, S.W. Boese, D.B. MacGowan, and F.P. Miknis, 1993, Simulation of hydrocarbon source rock maturation by hydrous pyrolysis, *in* B. Stroock and S. Andrew, eds., Wyoming Geological Association Field Conference Guidebook, Casper, Wyoming, p. 359-374.

Zeikus, J.G., and M.R. Winfrey, 1976, Temperature limitation of methanogenesis in aquatic sediments: Applied and Environmental Microbiology, v. 31, p. 99-107.

ISBN 1-884589-44-8